Synthesis and Characterization of Carbon Nanofiber Sheet Reinforced Polyvinyl Alcohol (PVA) Composite

A Thesis

Presented to

the Faculty of the Department of Mechanical Engineering

University of Houston

In Partial Fulfillment

of the Requirements for the Degree

Master of Science

in Material Engineering

by

Sicong Sun

December 2014

Synthesis and Characterization of Carbon Nanofiber Sheet Reinforced Polyvinyl Alcohol (PVA) Composite

Sicong Sun

Approved:

Chair of the Committee
Li Sun, Associate Professor
Mechanical Engineering

Gangbing Song, Professor
Mechanical Engineering

Cunjiang Yu, Assistant Professor
Mechanical Engineering

Suresh K. Khator, Associate Dean,
Cullen College of Engineering

Dmitri Litvinov, Professor, Director
of the Materials Engineering Program

Acknowledgements

First, I would like to thank everyone who helped me with my research and life, who made this thesis possible.

I would like to express my sincere gratitude to my advisor, Dr. Li Sun, for his guidance, encouragement, and support in my master research. His devotion to research and commitment to excellence motivate me to find my own path in my future research and work.

I would also like to give special thanks to my committee members Dr. Gangbing Song and Dr. Cunjiang Yu for taking the time to review this work.

I wish to give thanks to Min Lu, Christopher Ortega, Xiaodong Yu, and other members of the group for their time to discuss and solve the problems in this project. I would also like to acknowledge Dr. Haleh Ardebili and her group members Qin Li and Mengying Yuan, for their generous help with the test devices.

The most important, I would like to express my deepest gratitude to my family.

Synthesis and Characterization of Carbon Nanofiber Sheet Reinforced Polyvinyl Alcohol (PVA) Composite

An Abstract

of a

Thesis

Presented to

the Faculty of the Department of Mechanical Engineering

University of Houston

In Partial Fulfillment

of the Requirements for the Degree

Master of Science

in Material Engineering

by

Sicong Sun

December 2014

Abstract

Carbon nanofibers (CNF) reinforced polymer composites with lightweight, sustainability of large deformation, oil and corrosion resistance can have positive impact on a wide range of applications. However, this type of composites is still under extensive research due to the difficulties in material handling and processes scale up. To improve processing control and reproducibility for large-scale engineering applications, cost effective carbon nanofibers (CNFs) in form of interconnected porous sheet (Buckypaper) were used as nano fillers. Microstructure of fiber sheet and composite, static mechanical and dynamic mechanical properties of CNF reinforced polyvinyl alcohol (PVA) have been investigated. The effect of dimethyl sulfoxide (DMSO) solvent has been compared to water and shows better improvement in wetting and forming covering layer on the carbon surface. Our sample fabrication technique forms a layered structure where the interfacial debonding between outside PVA layer and inner composite layer can lead to negative impact on static mechanical property. However, the static Mechanical measurements on the composite samples still show significant modulus enhancement that doubles that of pure PVA with the same fabrication process and condition. DMA and DSC measurements show that the unique sandwich-like composite samples have improved storage modulus changing T_g of PVA.

Table of Contents

List of Figures

List of Tables

Chapter 1: Introduction

The innovation and application of materials is directly a mirror for the evolution of civilization. The stone-tipped spear from Neolithic age and a modern high performance electronic device are both examples of materials and tools for human beings. The materials can categorized into three different kinds based on their distinct physiochemical properties: metal, organic and ceramic. Through the long history of human civilization development, we learn to first utilize natural materials to meet our basic needs, and then learned to improve the properties of these materials and finally develop artificial materials that are not existed in nature. With the acceleration of science and technology, we found more and more limits imposed by existing materials, and the pursue of a higher level of performance has become the driving force for modern materials science and engineering. For example, traditional metallic and ceramic materials are now being replaced by more and more composite materials since the composites are able to combine the advantages from a variety of components and often process new properties that are not appeared in any of the individual components. For composite materials, based on the fraction of each component, we normally separate them into the matrix and filler material. The properties of the composites depends on a variety factors include the filler type, size, matrix material, distribution and geometry[1].

One of the most significant families for composite materials called the Advanced Composite Materials. They are initially developed to meet the rigor requirements for modern aerospace shuttle and electronic equipment industries. These materials are usually light weight with outstanding mechanical performance, and stability and high resistance to extremely physical chemical environment[1]. Among them polymer matrix

composites (PMCs) is one of the most important and fast developing type of advanced composite materials. Starring from 1970s, the application of PMC first emerged in aerospace and military applications and was then gradually expanded to automobile, sport equipment and consumer products. With almost 50 years of development, the application of PMCs has now extended to other areas such as biomedical, textile and electronic industries.

Initially the fillers used in PMCs are mostly continuous fibers such as the high-stiffness glass and aramid, but now new fillers such as the carbon fiber, carbon nanofibers, carbon nanotubes, nanoclays and nanoparticles are used. Carbon nanocomposite is an innovative research hotspot now in improving mechanical, thermal and conductive properties of polymers. Carbon nanomaterials such as carbon nanofibers (CNF), carbon nanotube (CNT) and graphene has distinct properties due to their nano size and unique structures-- can introduce high interface area/volume ratio with polymer matrix and their intrinsic high modulus, high thermal and electrical conductivity can greatly change polymer properties[2]. Since the nanocomposites are the most possible alternatives to the traditional materials in future civilization evolution, the more specific application polymer based nanocomposites developed to meet the requirement for variety circumstances. These new composites expected to be low cost, easy to manufacture and environmental friendly.

In this study, we focus the research on CNF reinforced polyvinyl alcohol (PVA) nanocomposites. The carbon nanofibers, has been made into a buckypaper form, are used as the reinforced and their effect on both the static and dynamical mechanical properties were evaluated. Different synthesis methods been employed and their effects were

investigated. The interactions between the carbon nanofibers sheet and PVA polymer were characterized and evaluated based on mechanical properties test, furthermore, the morphology of the composites were also studied to provide information on composite microstructure.

The thesis divided into five sections: Chapter 1 is introduction; Chapter 2 will cover the literature review of carbon nano materials, polymers and polymer nano-composites. Different polymer-carbon nanocomposites synthesis techniques also summarized and compared in this chapter. Chapter 3 summarizes the experimental methods, devices and techniques used in this study. Chapter 4 describes the research results and includes the discussion on observations. Finally, the conclusion and future work provided in chapter 5.

Chapter 2 Background/Literature Review

2.1 Carbon Based Nano-Materials

Carbon is abundant on earth and the most basic element for life. Apart from being the fundamental block of organic molecules, pure carbon can exist in a variety of structures. These so-called allotropes include diamond, graphite and charcoal. Charcoal, as a mineral, has be the main form of energy source throughout the human history. Its early applications also include medical use by the Egyptians and Sumerians dated back to 3750 BC[3]. Graphite has an even longer recorded application history: Boian culture used graphite in a ceramic paint in 4th millennium B.C. The wide application of nature graphite and artificial graphite has accelerates the development metallurgical and printing industry in 19 century. In 1950s, graphitized micro-diameter carbon fibers have been fabricated for aerospace and military applications[4]. The last decade of the 20th century experienced a dramatic increase carbon research when a new family of carbon allotropes including the C_{60}, carbon nanotubes, carbon nanofibers and graphene have been f. These carbon nanomaterials considered as the future of materials. C_{60}, also named as the Buckminsterfullerene/buck-ball was first discovered by Harold Kroto and Richard Smalley in Rice University in 1985. 1991, NEC scientist Iijima first time observed the carbon nanotube under the high-resolution transmission electron microscopy (HRTEM) when he evaporate the graphite electrode by using vacuum arc[5]. In 1993, the same NEC research group[6] and IBM[7] synthesized the signal-wall carbon nanotube by add the transition metal as the catalyst during the arc discharge. Also in 1993, Yacaman

successful obtained the multi wall carbon nanotube by using a chemical vapor deposition method, which allows better control of carbon nanotube growth[8].

Due to their unique structures, these carbon nanomaterials possess unique mechanical, electrical property and optical properties that are different from other bulk materials. Their lightweight and small sizes also made them the obvious candidate in improving current material performances and developing new applications.

2.1.1 Fullerene

Fullerenes are generally defined as "any of a class of hollow aromatic carbon compounds that are made up of twelve pentagonal and differing numbers of hexagonal faces[9]." Which means that, each molecule in the fullerene family, the number of carbon atoms should conform to Euler's theorem: m-(n-20) 2-1. The fullerene family includes a serial of stable carbon structures with C60 being the most famous one.

C60 named as the buckminsterfullerene after an American architect Buckminster Fuller, who designed the geodesic dome in 1960's. Few years after the discovery of this carbon nanostructure, in 1990, W. Kratschmer and D.R. Huffman[10] proposed a method to prepare macroscopic quantities of this material by initiating an arc between two graphite electrodes in a helium atmosphere. The member of carbon atoms in the fullerene family includes C_{60}, C_{76}, C_{78} and C_{84}. C_{60} have 12 pentagons and 20 hexagons; C_{70} consists of 37 faces, of which 12 are pentagons and 25 are hexagons. The C-C bond in C_{60} has two forms but there are eight different types bonds in C_{70}.

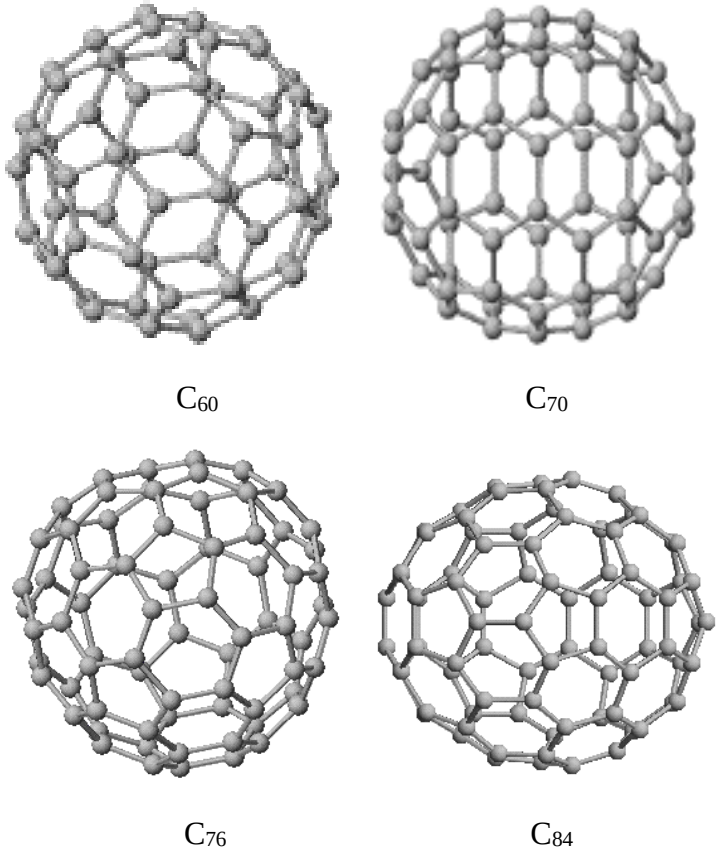

C_{60} C_{70}

C_{76} C_{84}

Figure 2. 1 The structure of members in fullerene family

2.1.2 The application of fullerene

Due to the unique structure of fullerene, the fullerene has drawn lot of initial attention from chemists. For example, C_{60} contains 30 π bonds that are chemically reactive, and the double bond between two carbon atoms are highly active. Chemists have been able to develop a variety of polymer derivatives from the fullerenes. These include the dendrimeric, fullerene-containing copolymers and star-shaped fullerene materials. Its electrical conductivity and chemical stability also makes the fullerene an idea electrode materials for organic light emitting device and electrodes[11]. Researchers have also tried to dope the C_{60} with boron and nitrogen to form materials such as $C_{59}N$. Its cage structure also allows researchers to embed other materials for developing new

contrast agent or drug delivery systems. Recently, there is also reports on using C_{60} to restrain cancer cell metastasize[12]. In summary, fullerenes as the first discovered carbon nanomaterial have shown perspective applications in battery, display, catalyst and new medical area.

2.1.3 Carbon Nanofibers

Carbon nanofibers (CNF) is one type of quasi-one dimensional carbon filaments. The diameter of current mass produced carbon nanofibers is normally around 50-200 nm, they are much bigger in diameter than the single wall carbon nanotube (SWNT) but similar to most of the multi-walled carbon nanotubes (MWNTs) and much smaller than the continuous carbon fiber. This property of CNF is also in the transition region between the micro-fiber and carbon nanotubes. A closer look at the atomic structure of the CNF shows its differences from the CNTs: the carbon nanofibers are solid internally and the graphite layer is not parallel to the axis. The angle between the layer and axis can vary depending on the synthesis method. As show in figure 2.2 CNFs can be regarded as regularly stacked truncated conical or planar graphene layers along the filament length[13]. It is a pure carbon (Carbon content is more than 90%) and has graphite lattice structure[14].

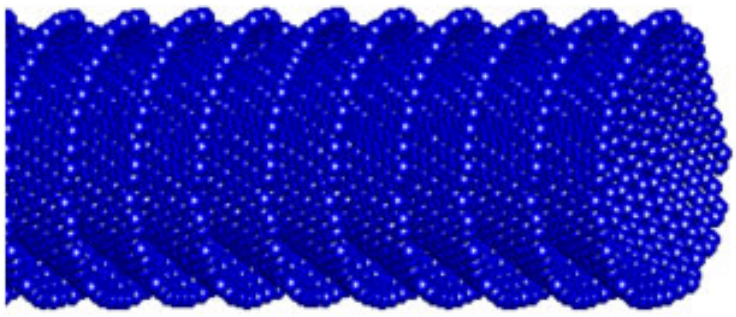

Figure 2. 2 The structure of carbon nano fiber

Due to its high aspect ratio, flexibility, high mechanical strength, high electrical conductivity and compact structure[15], CNFs can introduce unique properties to polymer matrices when compared to micron-carbon fibers. Due to its chemical properties and large surface area, they can also be used as catalyst or as a carrier for catalysts[16, 17]. CNFs applications as the anode in Li-ion battery[17], capacitor electrodes[18], catalytic membranes[19] and electromagnetic wave adoption materials[20] have been extensively explored.

2.1.4 Synthesis of Carbon NanoFiber

Scientists have already developed several methods for CNFs production. First, P.V. Adhyapak and colleague proposed to synthesize carbon nanofibers electrochemically[21]. They obtained the carbon nanofibers on a molybdenum electrode by cathodic decomposition of chloroform the room temperature. The carbonaceous material they got contains 24% Carbon fibers. Y. Matsumoto[22] and others fabricated carbon nanofibers by a hot filament assisted sputtering method. The carbon thin film been deposited on a substrate from a graphite disk target in argon gas. The final film was not composed of isolated carbon nanofibers but considered as a new type of nano-scale carbon fibrous crystallites.

More researchers synthesized carbon nanofibers by modified chemical vapor deposition methods (CVD). Fumiyuki Hoshi and coworkers[23] successful obtained carbon nanofibers at 550℃ by an electron cyclotron resonance enhanced CVD (ECR)-CVD. The deposition happened on a Si substrate coated with Ni catalyst and methane gas provided as the carbon source. B.B.Wang[24] also reported a method of growing carbon nanofibers by a negative bias enhanced hot filament CVD under glow discharge. The reaction mixed

gas contains CH_4, NH_3 and H_2. The aligned carbon nanofibers grow on a silicon wafer that already had a layer of NiFe and a Ta buffer layer. Both teams got high quality carbon nanofibers by these modified CVD method.

Now chemical vapor deposition is the most common and convenient method of producing nanofibers. The dimension and structure of the final products can be different depending on the catalysts and how they were added[25]. The general procedure to synthesis carbon nanofibers by CVD include following steps:

1. Silicon wafer or other high temperature resistant substrates will put into the CVD chamber.

2. After removing air from the CVD chamber, carrier gas flow will connect to the CVD chamber and heating to appropriate temperature.

3. The carbon source flow will connect to the chamber to replace the carrier gas flow under stable flow rate, pressure and temperature. The deposition process begin.

4. After the deposition, the carbon source flow will terminated and replace by argon flow during the cooling down process.

The carbon nanofibers obtained by this method called the vapor grown carbon nanofibers (VGCNF).

However, due to the limited yield, these methods most used in laboratories for research and development purposes. The most efficient way to prepare CNFs at an industrial scale is to use the floating catalyst method[26]. The schematic of the method shown in Figure 2.3. The reactor tube, usually made of quartz, has placed in a furnace. The carbon source and catalyst vapor connected to the reactor through the inlets installed at the top part of the reactor. The carbon fiber and exhaust gas come out from bottom of

the reactor. Generally, the catalyst precursor heated in a connected container. The carrier gas, mostly, H_2, will transport the catalyst to the quartz tube, as well as the carbon source vapor. These catalysts will decompose and form ions at high temperature and can uniformly dispersed inside the reactor. Many research groups used ferrocene as the catalyst precursor. Lijie Ci[27] used a liquid containing ferrocene as the precursor to ensure the Fe clusters could be fully generated and got in contact with carbon at high temperature. Jipeng Cheng[26] used aerosol ferrocene as the precursor to get high quality substrate-free carbon nanofiber bundles. The floating catalyst method has much higher productivity than other methods due to its continuous operation capability and the distribution of nanoparticle catalysts also better, which can lead to high quality product. It has also become the industrial level manufacture technique for one-dimensional carbon allotropes.

Besides the floating catalyst CVD method, some researchers tried to use a template synthesis method or seeded catalyst method to prepare the carbon nanofibers. The substrate will seeded or covered by a layer of catalyst then put into the CVD chamber or reactor. Hans Jaegar and Tom Behrsing[28] added the iron particles as catalyst to the alumina substrate. G. Che[25] prepared the nickel catalyst on substrate by heating an organometallic nickel membrane. These methods are capable of fabricating better controlled and most of the time aligned CNFs, but they are normally less efficient and hard to scale up to a continuous manufacture process.

There are other attempts to cut the CNF manufacturing cost with large-scale production capability. Munehiro Ishioka[29] fabricated CNFs using gaseous CO-CO_2-H_2 as the carrier gas and utilized benzene solution containing ferrocene and cobalt-

acetylacetonate as the catalyst precursors in the gas flow. However, the catalyst distribution is not uniform and the final product contains only a small percentage CNFs with low quality.

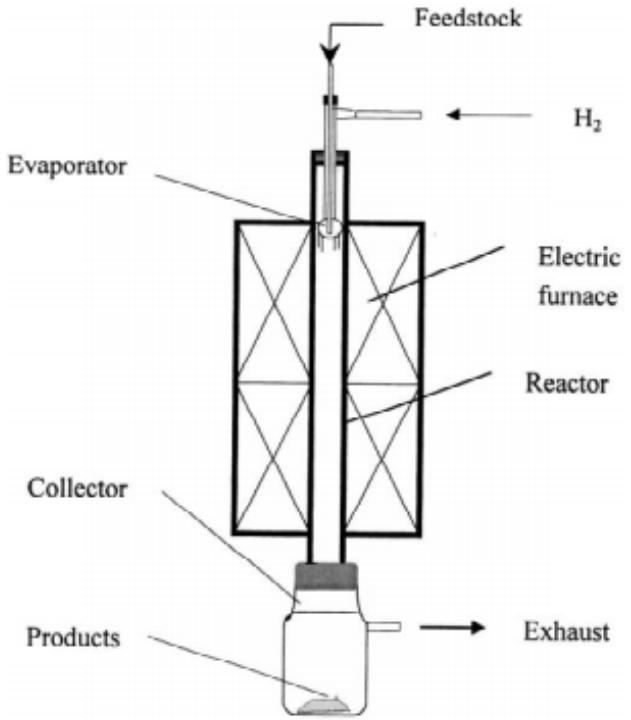

Figure 2. 3 Schematic of floating catalyst method CVD to growth carbon nanofibers[27]

The morphology of carbon nanofibers can also be different caused by different growth conditions and using different kinds of catalysts in the CVD process. X. H. Chen[30] and coworkers obtained segmented graphite nanofibers by using a foam Ni catalyst under acetylene carbon source. The carbon nanofiber obtained by A. Oberlin and M. Endo[31] had turbostratic stacks and arranged in “annual ring structure” when they pyrolysing a mixture of benzene and hydrogen. Nelly M. Rodriguez[13] found two different kinds of carbon nanofiber structures: Layer by layer stacking and herringbone stacking using different catalysts.

2.1.5 Carbon nanotube

There is yet another member of the fullerene family: carbon nanotubes, also called Bucky tubes, which are quasi one-dimensional, sp^2 hybridized carbon materials. The number of graphene layers rolled up determines the radius of these hollow tubes. There are two kinds of carbon nanotubes: the SWNTs and MWNTs. The single wall nanotubes can be thought to be formed by rolling a one atom thickness single layer graphite (graphene nanoribbon) into a seamless tube with specific angles[32]. The multi wall nanotube is the nesting of single nanotubes. Usually both ends of nanotube capped with half-sphere fullerene molecules.

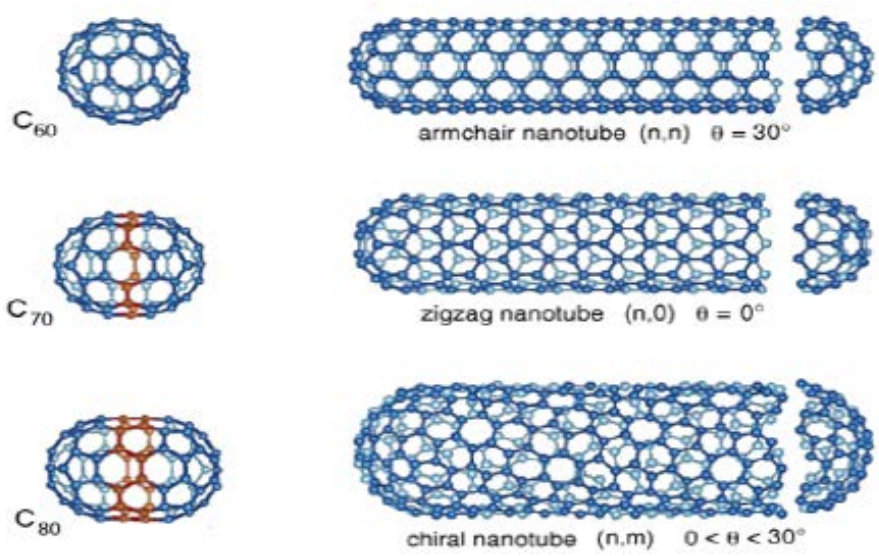

Figure 2. 4 Different types of carbon nanotube and their capping structure respectively

Depend on the roll-up angle, three different single wall nanotubes can be identified: the armchair SWNT, the zigzag SWNT and the chiral SWNT. They can also have different capping fullerene molecules. The chiral angle is helps to categorize the carbon nanotubes. As shown in figure 2.5, $\vec{a}$ and $\vec{b}$ are the unit vectors for a graphene

lattice, every hexagonal unit cell contains two carbon atoms (A and B). The chiral vector $\vec{L}$ determine the structure and gives the circumference. It can defined as

$$\vec{L} = n\vec{a} + m\vec{b} \qquad n, m \text{ are integers,} \qquad (2.1)$$

η is denoted as the chiral angle. a $= |\vec{a}| = |\vec{b}| \approx 2.49$Å , there are three scenarios here:

When $n = m$, chiral vector $\vec{L} = n(\vec{a} + \vec{b})$, $\eta = 30°$ and defines armchair carbon nanotube;

When $m = 0$, chiral vector$\vec{L} = n\vec{a}$, $\eta = 0°$ and defines the zigzag carbon nanotube;

When $0° < \eta < 30°$, it defines the chiral carbon nanotube.

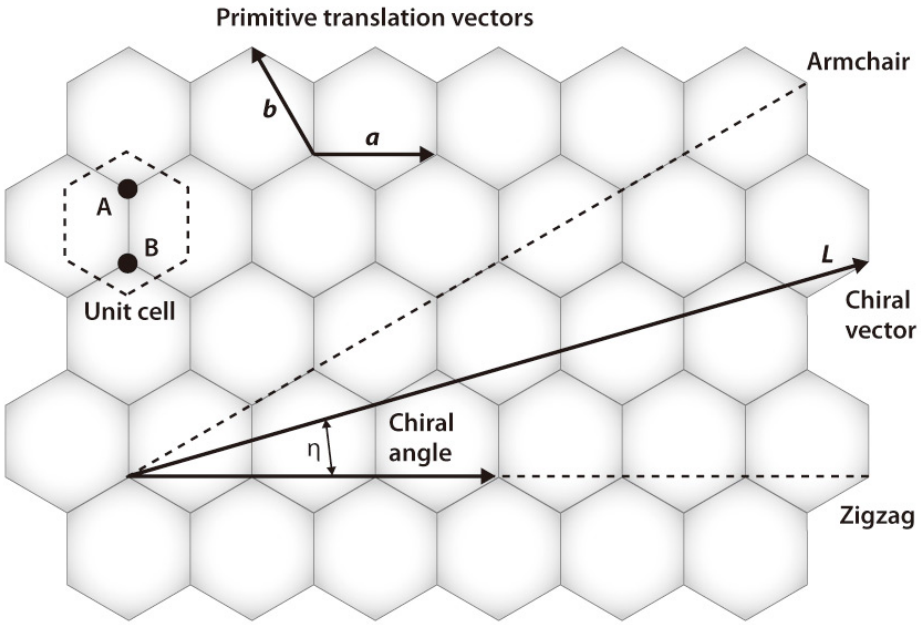

Figure2. 5 The honeycomb lattice of graphene and the illustration of different types of carbon nanotube[33]

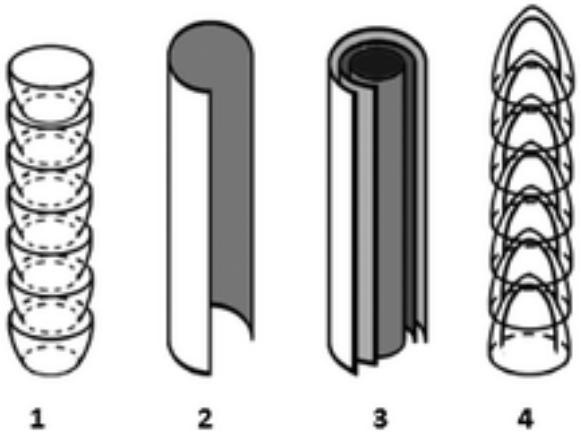

Figure2. 6 Structure differences between 1 carbon nanofiber, 2 single-walled carbon nanotubes, 3 multi-walled carbon nanotube and 4 bamboo carbon nanotube[34]

MWNTs have similar base structure as the SWNTs, they can consider as the nesting of several SWNTs with different diameters. The distance between neighboring tubular layers is approximately 3.4 Å, which is little larger than the distance between two layers in graphite. In a sense, carbon nanofibers are a kind of extreme multiwall carbon nanotubes. Figure 2.6 shows the structural different between four different kinds of one-dimension carbon nanomaterials. 1 is a carbon nanofiber, 2 is a single wall carbon nanotube, 3 is a multi-walled carbon nanotube, and 4 is a bamboo-like carbon nanotube, which can be obtained via microwave plasma enhanced CVD growth. The local concave and convex happened caused by tension when pentagons and heptagons appeared in honeycomb graphite lattice[32].

2.1.6 Synthesis and application of carbon nanotube

The carbon nanotube (SWNT &MWNT) can synthesize by similar methods used for as carbon nanofibers. The only differences in conventional CVD type of synthesis

methods are specific growth parameters or choice of catalysts. Besides the CVD method, there exist some other methods for CNT production.

2.1.6.1 Electric Arc Discharge Technique

Carbon nanotubes were first synthesized via electric arc discharge by Iijima[5]. In this method, carbon nanotubes generated on negatively biased electrode under a DC arc-discharge in an argon-filled vessel. According to the research from T.W. Ebbesen and P.M. Ajayan[35], by optimizing the voltage and current density used in arc discharge, the helium gas pressure, and choosing high purity graphite electrodes, it is possible to increase nanotube yield. In these experiments, the distance between two electrodes were kept between 1~2 mm. A temperature of 2000-3000^{o}C is needed at the core part of the cathode for carbon nanotube formation. The electric arc system showing by figure 2.7[32, 36].

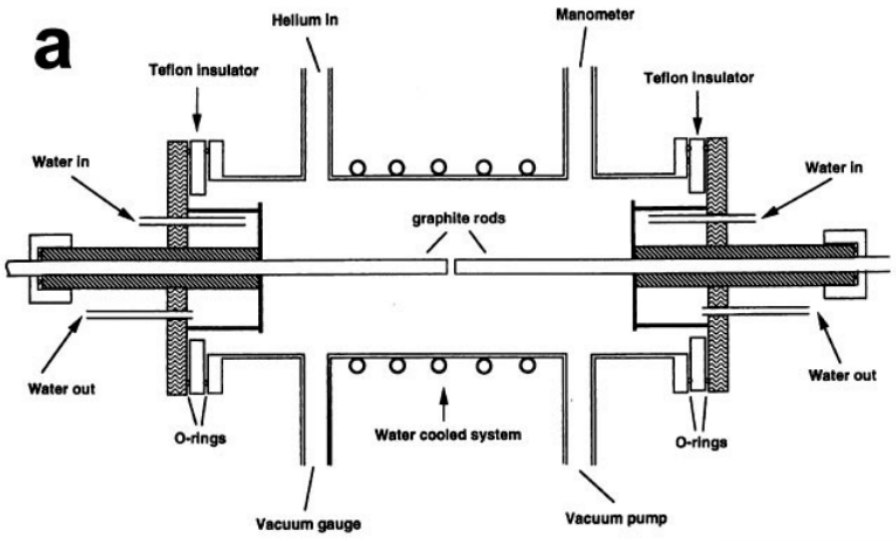

Figure2. 7 Schematic of electric arc device for carbon nanotube fabrication[36]

Besides the MWCNT, Iijima and Ichihashi also synthesized SWCNT by this method[6]. They modified the electrodes by using an iron added carbon cathode at the bottom and a pure carbon anode above it. The experiment processed in a methane and argon environment. The iron evaporated under the arc and became the catalyst. People later found that using this method, SWNT can be produced with different metal catalysts including Co[37] and Co-Ni-Fe-Ce[38]. Yoshinori Ando proposed a new approach to obtain large quantities of SWNTs by using DC arc plasma jet (APJ) method[39].

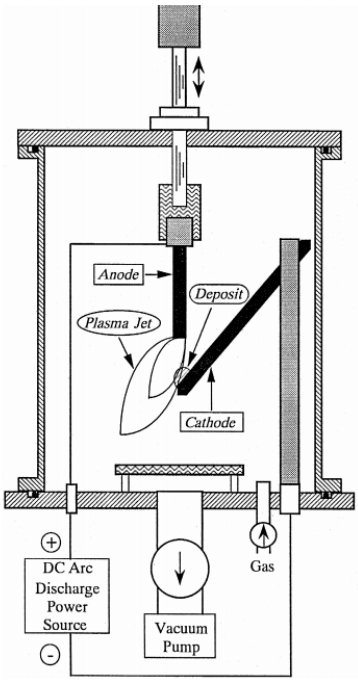

Figure2. 8 Schematic diagram of the DC arc plasma jet (APJ) apparatus[39]

The APJ system show by figure 2.8. Arc plasma jet formed between catalyst doped carbon anode and oblique cathode under DC voltage and 60 A current. SWNTs generated in plasma region and collected by the substrate. However, the high purity

graphite electrodes in this system make this method to be more costly when yield is same as other methods.

2.1.6.2 Laser vaporization

Laser vaporization, also caller laser ablation, uses high power pulsed laser pulse or continuous laser to vaporize a carbon target and carbon nanotubes can be collected at a cooled collector[40]. The Process of the laser vaporization showed in Figure 2.8. In this method, a solid graphite target containing catalyst is used and argon normally used as the working gas. The setup placed in a tube furnace. During the laser ablation process, the bulk carbon in the target will be converted to vapor and diffuse along the temperature gradient in furnace, carbon nanotubes can nucleate and grow in the vapor and being carried away by the argon flow and finally condensed on the Cu collector[41]. In order to generate SWNTs, the carbon target needs to contain a small amount of metals such as cobalt and nickel as the catalysts. Thess[42] demonstrated the synthesis of SWNTs by using Co-Ni-graphite mixed target. SWNTs can also been synthesized without furnace when using a continuous CO_2 laser. The target should be placed vertical to the inert gas flow and the laser can heat the target surface[41]. This method is much for expensive than the electric arc discharge technique and yield is also low.

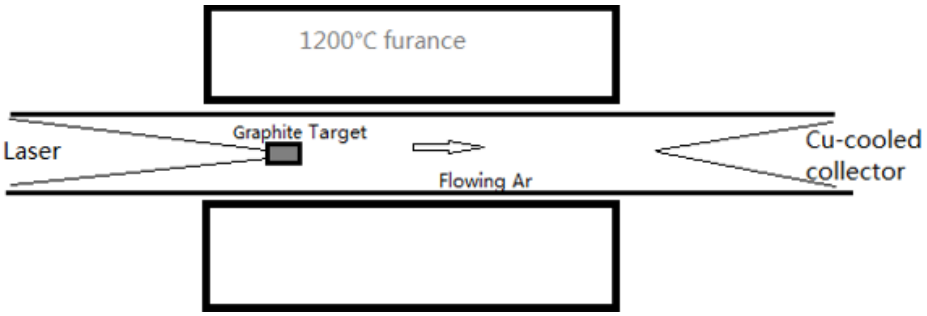

Figure 2. 9 Schematic of laser vaporization device for carbon nanotube fabrication

2.1.6.3 Solar beam Vaporization

Solar energy has also directly used to synthesize CNTs. Instead of using an electric tube furnace, the sunlight can be collected first by flat mirrors and then a parabolic mirror to focus on a carbon-metal target in an inert atmosphere[43, 44]. D. Laplaze[44] and coworkers succeeded in obtaining both SWNT and MWNT using this method under different experimental conditions. As shown in Fig 2.9, a graphite target containing metal catalyst placed in the middle of furnace and with the focus of light; the temperature could rise above 2800K in a sunny day. This temperature will evaporate carbon and catalyst and similar carbon nanotube growth as laser vaporization will take place. CNTs deposit on the cold surface then be collected. There are many efforts in scaling up this process by using high-density solar flux to improve the quantity of products. T. Guillard[45] improved the solar flux to 920 W/cm^2 and generated the mixture of fullerenes and nanotubes.

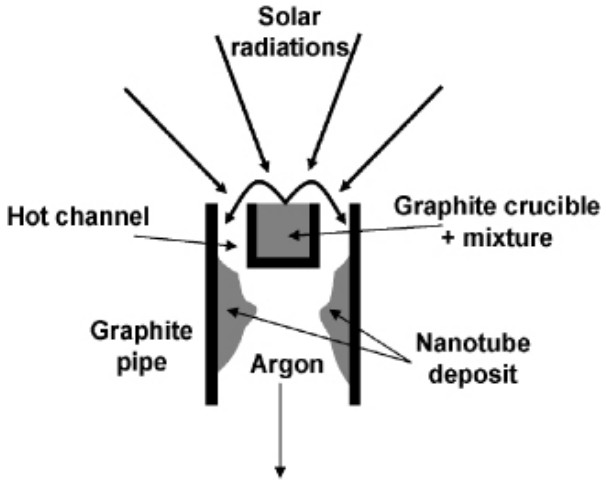

Figure2. 10 Schematic of solar beam vaporization device for carbon nanotube fabrication

2.1.7 Buckypaper

Carbon nanotubes can make into sheet form that also called the Buckypaper. It is first reported by the Smalley group[46] in the process of purifying SWNTs. This thin sheet of SWNTs is made of intertwining nanotubes holding together by the Van der Waals interaction. Buckypapers are porous and freestanding. Assemble CNTs or CNFs into Buckypaper greatly enhance the handleability of nanomaterials and large scale engineering application of CNTs and CNFs possible[47]. Also these Buckypaper have superior mechanical and electrical properties that can extend the carbon materials applications in super capacitors[48], solar cells[49], Li-ion batteries[50] and fuel cells[51]. In this study, we will focus on study the mechanical enhancement in polymer matrices.

2.1.7.1 Fabrication of Buckypaper

The general methods of fabricating Buckypaper include a two- step method and a one-step method. The two-step will have the carbon nanomaterials synthesized first and then make them into a paper form. One the other hand, in the one-step method, the Buckypaper directly made directly from CNT/CNF grown on substrate. In the first report on Buckypaper in 1998, Jie Liu developed the buckypaper by using SWNT suspension filtrated through a polytetrafluoroethylene filter membrane[46]. Before the filtration process, the SWNT has purified by nitric acid to eliminate other species such as amorphous carbon then made to an SWNT suspension with a pH of 10. Later, Whitby[47] also successfully obtained Buckypaper of MWNTs which were purified by using high temperature heating and hydrochloric acid treatment.

The generation process of the filtration-fabrication of Buckypaper includes:

1. Preparation and purification of carbon nanomaterials. Normally high concentration acid used to dissolve any impurities such as amorphous carbon, other spheroidal fullerenes, and the catalysts during CNT/CNF fabrication.
2. Dispersing carbon nanomaterials in a solvent to make suspension. Surfactant such as Triton X-100 and sodium dodecyl sulfate e usually used as dispersing agent and ultra-sonication process often employed to obtain a uniform suspension.
3. Filtration of suspension. Porous Polytetrafluoroethylene (PTFE), polyvinylidene fluoride (PVDF), Nylon or polycarbonate (PC) membranes are used to filtrate the liquid and collect Buckypaper.
4. Drying in vacuum oven and Buckypaper can peeled from the filtration membrane.

This dispersion and filtration method is very facile and highly efficient in making buckypaper with required thickness. However, CNT/CNF can aggregate during the filtration process, and the buckypaper synthesized by this method tends to have weak mechanical strength. In addition, the existence of residual surfactant can affect the electrical and thermal conductivity of buckypaper.

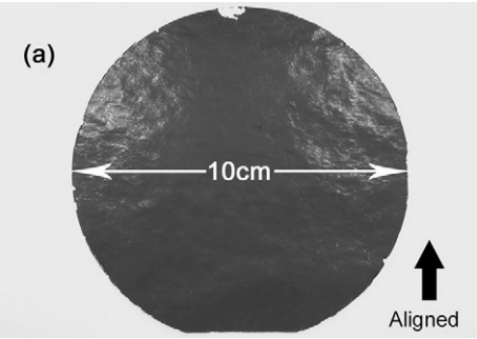

Figure2. 11 Planar Buckypaper with aligned carbon nanotube

A research team from Tsinghua University developed a dry method to fabricate aligned carbon nanotube papers[52]. In the process, CNT array first grown on silicon substrates. A microporous membrane then directly placed on the CNT array and a cylinder was pushed to roll on the CNT array and force them to incline along one direction and form buckypaper. The buckypapers made by this method have good mechanical strength and electrical conductivity. However, the yield of the method limited by CVD growth of CNT/CNFs on the substrate, and the tuning of buckypaper properties of mixing different carbon nanomaterials are difficult to achieve.

Recently, there are other efforts to fabricate buckypaper. Hiroki Ago[53] fabricated buckypaper via spin coating. Purified MWNT suspended in liquid and directly spun coated on glass or quartz substrates to form buckypaper. The thickness of the buckypaper adjusted by controlling the MWNT suspension concentration and spinning speed. The buckypaper synthesized by this method could be thin and flat. However, this method is more complex than filtration and large size buckypaper are difficult to make.

Buckypaper fabrication by directly growth has also been experimented. Ruitao Lv[54] increased the CNT growth time during a conventional CVD process, in which Ar and H_2 were used as the carrier gases for ferrocene catalyst and carbon source. The extended growth time allowed CNT entanglement and direct formation of an interconnected structure. The buckypaper fabricated by this method can easily peeled off from the quartz substrate. In another experiment, Lijie Ci[55] first deposited an iron catalyst layer on aluminum coated Si wafer followed by CVD fabricating of buckypaper. By using ethylene as carbon source and an argon, H_2 and H_2O mixture as carrier gas, the synthesized buckypaper can self-separated from substrate.

2.2 Polymer Science

2.2.1 History of polymer science

"Polymer" is part of human life since the beginning and all life forms contain polymeric molecules. Protein and starch are nature polymers existed in food. Wood and bamboo are nature polymer composites used by human as construction materials. Paper, considered as the greatest invention in early 2nd century AD is also a kind of nature polymer material. For a very long time the polymeric materials used are limited to these natural materials such as the papermaking, leather tanning and painting industry. It is not until the middle of 19 century, people start to study the chemical modification of nature polymers. In 1839, Charles Goodyear discovered the process of nature rubber vulcanization; as the first thermoplastic, Celluloids synthesized nitrocellulose and camphor in 1856; then French scientist Hilaire de Chardonnet invented the viscose fiber and built an industrial synthesis process at 1893. The first synthetic resin plastic-phenol formaldehyde resin (PF), also known as Bakelite, was obtained in early 20 century.

So people did not understand the concept of polymer, let alone the molecular structure and configuration of polymer, until 20th century. In 1920s, German chemist Herman Staudinger proposed the famous polymer hypothesis: The rubber and other polymers like cellulose are formed by long chains containing numerous repeat units. Until then scientists began to understand the structure of polymers and their characteristics. Between 1920s and 1940s, the study of polymerization led to the synthesis of a family of artificial polymers, including Polyvinyl Chloride (PVC), Polystyrene (PS) and Poly (methyl methacrylate) (PMMA)[56]. These polymers can have very different properties to fulfill different application requirements. In 1935, Nylon 66[57]

was invented, which is considered the beginning of the plastic era. A polymer boom took place in 1950s and 1960s[57]. The appearance of new polymerization technologies made it possible for people to develop new functional polymers such as high temperature resistance and high strength polymers[56]. High-density polyethylene (HDPE), Polyimide (PI) and Polycarbonate (PC) are some of the examples.

Development in polymer solution theory and polymer characterization methods in 1970s also greatly accelerate the growth of polymer industry. Nowadays, techniques such as nuclear magnetic resonance (NMR), Fourier Transform Infrared Spectroscopy (FTIR), X-ray Diffraction and Light scattering become widely available for us to study the physiochemical properties of polymers and polymerization processes[58].

Entering the 21st century, polymer industry continued on the research and innovation of differential functional polymers. Biocompatibility, ablation resistance, ultrahigh pressure tolerance, chemical/radiation stability and other requirements taken into consideration for modern polymeric material. Liquid crystal polymer[59] can biopolymer medicine have already improved our life and the volumetric production of polymer have far exceeded steel and metal production. Polymers are replacing conventional metallic and ceramic materials and meeting our needs for low cost, high performance, easy to maintain materials.

2.2.2 Poly vinyl alcohol (PVA)

Poly vinyl alcohol (PVA) is an artificial linear synthetic polymer. Figure 2.1 shows the structural formula of PVA. The synthesis of polyvinyl was first described by two German scientist: Herrmann and Haehnel, in 1924[60]. The side group-hydroxyl group

on the PVA chain make it highly soluble in water and other polar solvent. Besides, PVA has good film forming ability and is highly resistant to oil and other organic/inorganic solvents. PVA became commercially available in 1950s and it has extensively used as adhesive, emulsifier, binder, fibers, bases of photoresists, and protective colloid. It is also the main raw material for Vinylon fiber fabrication[61].

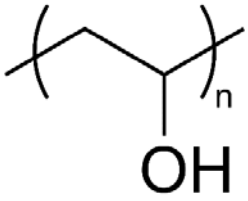

Figure 2. 12 Structural formula of PVA

2.2.2.1 Manufacture of Polyvinyl Alcohol

Unlike most polymers that obtained by polymerization of their monomers, poly vinyl alcohol cannot be direct polymerized by vinyl alcohol because it cannot exist in the free form. Instead, the PVA can formed by hydrolysis of polyvinyl acetate. Figure 2.12 shows the process of PVA formation during industrial synthesis.

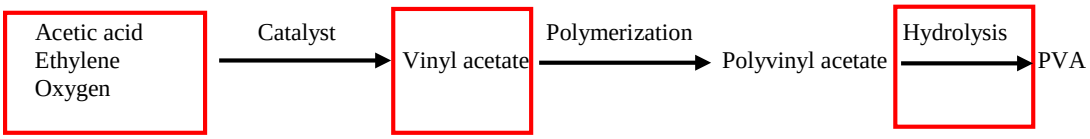

Figure 2. 13 Chemical configuration of PVA[60]

The polymerization of free radical chain of vinyl acetate usually takes place in organic solvent such as methanol. The presentence of methanol are necessary for several reasons:

1. Acting as a chain transfer agent and helping the initiator to adjust the molar masses of polymer chain to different values;
2. Removing the heat generated during polymerization by evaporation;
3. Participating in the hydrolysis process of polyvinyl acetate

The Hydrolysis reaction of polyvinyl acetate requires sodium hydroxide (NaOH) to act as the catalyst:

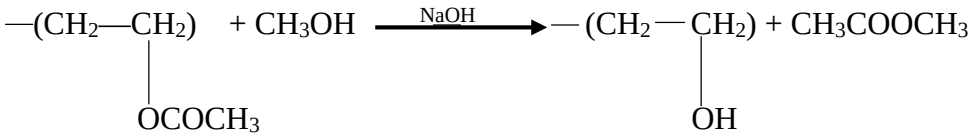

The degree of PVA polymerization determined by a variety of parameters: these include the concentration of catalysts, reaction temperature and reaction time. They will determine the residual acetyl group content in final product. In addition, after the alcoholysis, the sodium acetate need to remove.

2.2.2.2 The structure of polyvinyl alcohol

The reaction forming the polyvinyl acetate decides the structure of PVA chains. The hydrolysis process happens based on the structure of poly vinyl acetate, so if assuming vinyl acetate polymerization takes place the head-tail-head-tail form, the final PVA structure of PVA will be:

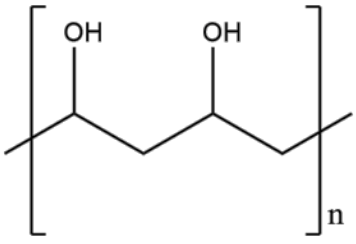

Figure 2. 14 Head-tail type PVA structural formula

Of course, if the vinyl acetate not only polymerizes in head-tail-head-tail form, but also takes the head-head-tail-tail sequence, then the final structure of PVA would be1,2-glycol, shown as:：

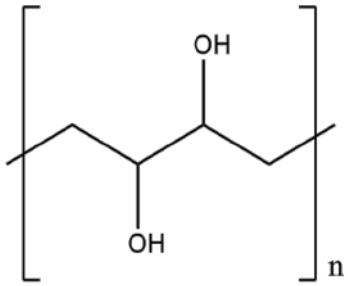

Figure 2. 15 Head-head type PVA structural formula

The properties of PVA will be affected by the structure of polymer chain-syndiotactic or isotactic. Generally, the syndiotactic chain growth has priority. The syndiotactic polyvinyl alcohol shows more resistance to water.

PVA can also dissolved in dimethyl sulfoxide (DMSO), but its solubility in the mixed DMSO/water and DMSO is much lower and gels can be formed. The maximum rate of gelation is observed for a liquid containing the solution of 60 vol % DMSO[60].

2.2.3 Polymer/Carbon Material Composite

Compsoite materials combine the advantages of different components. The modern composite materials are often designed and manufactured targeting specific functionalities. Based on the different types of matrix material, functional composites developed after 1970s are categorized into polymer matrix composite (PMC), ceramic matrix composites (CMC) and metal matrix composites (MMC). Among them the PMC are the most used composites with unsurpassable advantgaes in structure applications due

to their lighter weight, high specific strength and high specific stiffness and other physiochemical properties[1].

During the development PMCs, carbon based fillers have been found to have extensive application potential due to their unqiue structrue and superior properteis. Starting from carbon black and micro-diameter continuous fibers, fullerines, carbon nanofiber and carbon nanaotubes can all be used to advance polymer composite development[15]. The applications of carbon reinforced polymer matrix inclued but limited to aerospace indsutry, auto industry and energy industry.

2.2.3.1 Polymer/ Continuous Carbon Fiber Matrix

Continous carbon fibers are fabricated from graphitization of organic fibers using ogranic precursors. The most common precursors for continuous carbon fabrication are the Polyacrylonitrile (PAN) or mesophase pitch (MP)[62]. The common manufacturing processes are:

1. The precursor fiber is first stabilized and oxidized at 200-400℃ in air.
2. Stabilized carbon fiber will be heat treated at about 1000℃ in an inert atmosphere to achieve carbonization.
3. Graphatization can happened at higher temperature like 2000℃[63].

Finally carbon fiber products normally have least 92% of carbon and the diameter of these fibers is ususally between 5 and 10 μm[64]. Depending on the percursor and heat treatment condtions, the properties of continous carbon fibers can be different, but usually the have high tensile strength, good thermal and electrical conductivities and also

high chemical/thermal stabilities. The applications of carbon fiber can be traced back to 1950s. Carbon fiber–thermoset resin is the most commonly used composite system. Thermost resins often have low viscocity before curing and can be made into complicated shapes. Since the carbon fiber modulus can vary between 4 Gpa to 500 Gpa, and different resin system should be processed by different manufacturing processess. Commonly used resins are epoxy, phenolic resin, polyester resin, polyimides and bismaleimides[65]. Process methods for these resin usually include wet layup, vacuum bag molding, transfer moulding, pultrusion and autoclaving.

Boeing has recently build the entire fueslage and wings of 787 dreamliner from carbon fiber reinforced composite[1]. In addtion carbon resin matrix has also been applied to fabricate engine cowling and rudder. The total weight of the composite parts exceeds 70 percent and in volume terms passes 80 percent. The light weight of the composites is expected to improve fuel efficieny by 20 percent. Maintainence and repair cost is also expected to drop.

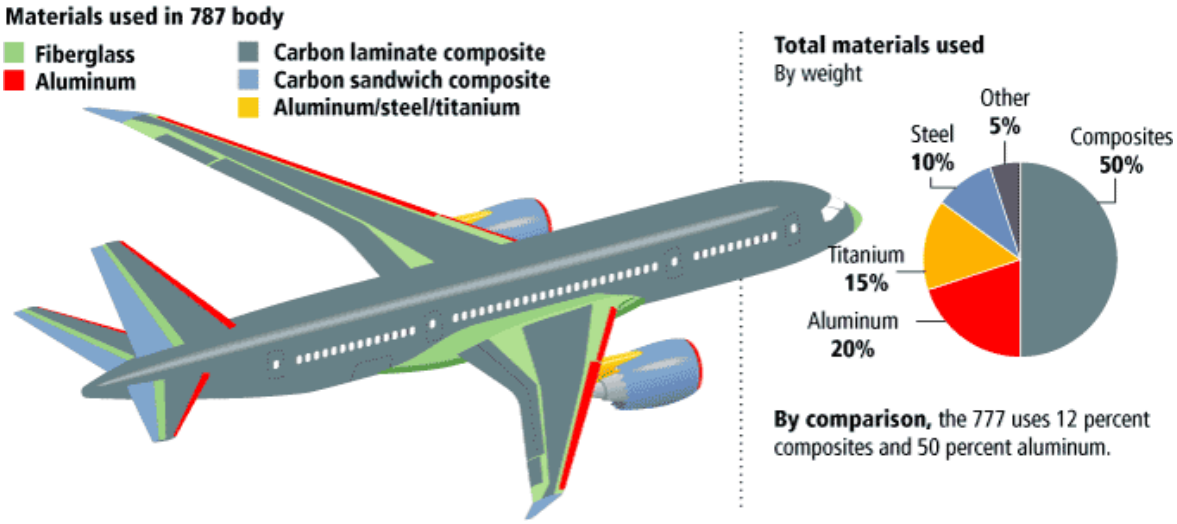

Figure 2. 16 Materials Application on Boeing 787

2.2.3.2 Polymer/Carbon Nanomaterial Composites

Carbon nanomaterials in general, are expected to have significant reinforcing capabilities due to their intrinic strength and high surface to volume ratio[15]. Compared to micron-daimeter continous carbon fibers, there loading conditions are totally different.

Table 2. 1 Typical properties of VGCNF, SWNT, MWNT and CF[66]

Property	VGCNF	SWNT	MWNT	CF
Diameter (nm)	50-200	0.6-0.8	5-50	7300
Aspect ration	250-2000	100-10000	100-10000	440
Density(g/cm^3)	2	~1.3	~1.75	1.74
Thermal Conductivity (W/m K)	1950	3000-6000	3000-6000	20
Electrical Resistivity (Ω cm)	1×10^{-4}	1×10^{-3}-1×10^{-4}	2×10^{-3}-1×10^{-4}	1.7×10^{-3}
Tensile Strength (Gpa)	2.92	50-500	10-60	3.8
Tensile Modulus (Gpa)	240	1500	1000	227

The tensile modulus of SWNT and MWNT can be three times higher than that of the CNFs. Yet in the nanomaterial reinforced composites, fillers take load from interface shear stress. So the filler-matrix interfaical bonding strength becomes more important than the intrinsic filler strength in determining the composite mechamical properties.

Because the interface bonding strength is expected to be much lower than the carbon nanomaterial strength, the reinforce effect of CNTs and CNFs should be comparable provided they have the same size and surface chemistry.

In comparison with continous fibers, nano reinforced PMCs can have better performances due to following three reasons:

1. Smaller diameter leads to high surface area/volume ratio, which also means more contact area for load transfer and interface dynamic energy dissapation ;
2. CNT/CNF with high flexibility and large aspect ratio can lead to improved PMC ductility. indicates fibers inside matrix can maintain aspect ration, which can give the matrix better mechanical property.
3. Interfacial defects density and size can be lowered.

After 60 years of research and development, continusous carbon fiber reinforced PMCs have been used in a wide range of applications including airplane, aerospace, vehicle, sporting, wind turbine blade, etc[62]. However, nanocarbon composites are still in their infancy and mostly still in the lab development stage, this is because nanomaterial handling, quality control, long term reliability and cost still remain as the major hurdles. But slowly and surely, nano-reinforced and functionalized PMCs begin to emerge in the market in recent years[67].

Carbon nanomaterials price depend on their purity, uniformity and quality. Compare to continuous carbon fibers (around $0.2 per gram), carbon nanofiber ($0.2-1.2 per gram) and carbon nanotube ($20-500 per gram for MWCNT and $375-2000 per gram for SWCNT) prices are much higher. But with major production expansion and

lower technical barrier, CNF and CNT are easily available[68]. In this study, we focus on the CNF-PVA nanocomposites.

2.2.4 Synthesis Methods for Polymer /Carbon Nanomaterial Composites

The synthesis of carbon nanomaterial/polymer compsite is not limited to the traditional mixing process anymore. Currently there are six types of nanocomposite processing methods.

2.2.4.1 Solution Processing

Due to the size of the nanomaterial, mechanical mixing is normally not effective, and the addition of CNT/CNF to the polymer will greatly increase the mixture viscosity and causes problems to mechancial mixing. So a widely adopted method to add CNTs or CNFs to polymer is using solution processing. The carbon nanomaterials are first dispersed in an appropriate liquid before mixing with polymer, which is normally also made into a liquid form. Aggregation of carbon nanomaterials is the most common and negative factor impacting composite properties, so the choice of solvent should reduce this aggregation. Solution processing method ususally includes three steps:

1. Dispersing CNT/ CNF in appropriate solvent;
2. Mix the CNT/CNF solvent with polymer solution by energetic agitiation (Temperature of mixing depend on chamical property of solvent and polymer).
3. Obtain the composite film by solution casting and evaporation rate control.

To improve nanomaterial dispesion in solution, external agitation in addtion to the simple stirring is often used. One commonly adopted practice is to use ultrasonication to break up nanomaterial bundle and achieve a metastable suspension of CNT/CNF using

locally generated shear force. Using suitable surfactant is another possible solution. For example Naoual Diouri[69] *et al* prepared several different concentrations of PVA/ SWCNT mixtures. They dispersed CNT in distilled water first using sodium dodecyl sulfate (SDS) as surfactant together with ultrasonication bath. After dissolved PVA in water, the mixture of PVA and SWCNT were then mixed fo 10 min using mechanical stirrer at elevated temperature. However, one disadvantage of using surfactants is it can retain in the compositeafter evaporation. This can affect the properties of polymer matrix and composite. One research team reported the thermal conductivity drop using sodium dodecyl benzene sulfonate (NaDDBS) as surfactant in SWCNT/epoxy system.

In addtion, CNT/CNF re-aggregation can happen during solvent evaporation and static evaportion of metastable suspension solution could also lead to precipitation of fibers. To reduce the evapostion time, several ways such as spin casting, drop-casting and vacuum evaporation were tested to shorten the evaporation time and reduce nanomaterial precipitation. For example, M.Cadek prepared PVA/CNT composite films by repeating the process of drop casting and oven evaporation. Everytime, 1 ml of suspension was droped on teflon disk each time then the sample is dried in oven. This method can be used to prepare uniform distributed film in short time.

2.2.4.2 Melt blending

Melt blending is an industrial scale manufacturing technique which has also been applied to nanocomposite farication[70]. The melting process includes the melting of polymer pellets to form a viscous liquid and with the application of high shear force when mixing with additives. Appropriate high temperature is very critical for lower the

visocosity of polymer matrix and achieve better distribution of additives when over high temperature could case degradation of polymer.

2.2.4.3 In-situ polymerization

By mixing the pre-polymer or monomers with CNT/CNF first, and the composites can be fabricated by in situ polymeration. The advantages of this method is it can achieve high level of uniformity in filler distribution. The polymer matrix and fillers normally can have a high level of integration and surface bonding[71]. But the addition of these nanoscale fillers can affect the polymerization proess of the matrix material and change the matrix properties.

2.2.4.4 Electro- spinning

Electrospinning-spun is a newly developed method to produce continuous composite fibers. It uses an electric field draw fine fibers from a liquid phase of polymer and filler mixtrue. Figure 2.17 shows the basic principle of electrospining. A high voltage is applied between the spinneret and collector. Liquid inside spinneret will be charged and the liquid droplet will be stretched. Once the repulsive force overcomes with the suface tension of liquid droplet, a fine liquid stream will be drawn from the tip (Taylor Cone) at constant flow rate towards the collector. The liquid stream will solidify when the solvent evaporates to form fibers[72]. When the liquid contains both polymer and nanofillers, composite fibers can be obtained.

Electro-spinning has been successfully applied to synthesize various polymer nanofibers and compsoite nanofibers. Fiber can be collected differently to form various composites. Rotating Mandrel can be used to collect aligned fibers. Flat metallic plate can be used to build random nanowoven mat. Naoual Diouri[69] prepared the PVA/CNT

nanofibers by the electro-spinning process. The CNTs-PVA mixtures was electrospun at15KV to form a 145 nm diameter composite fiber with 0.3% of MWCNT in PVA. J.S. Jeong[73] studied the mechical properties of electrospun PVA/MWCNT composite fiber. They collected the composite fiber by a rotating metal drum. They also obtained non-woven composite sheet by depositing the fiber on a plain substrate. The tensile strength of compsoite fiber is found to increase to 9.3Mpa, comparing to pure PVA, which only has a tensile strength of 5.8 Mpa.

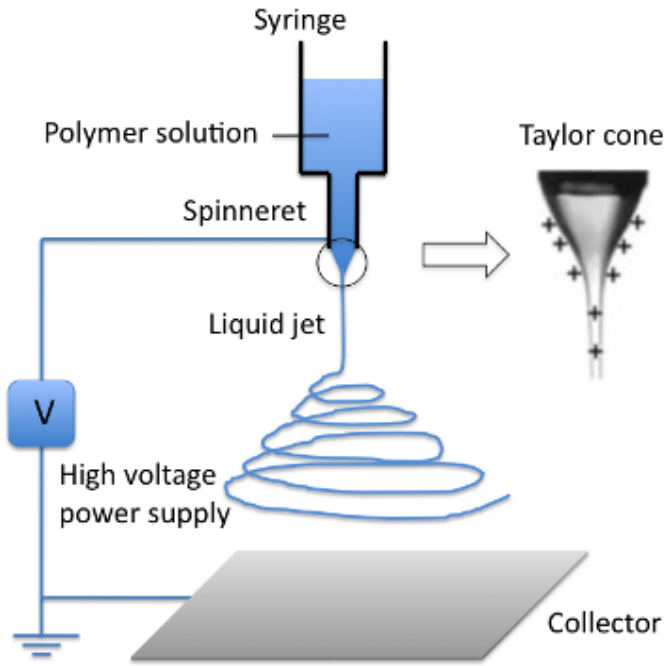

Figure 2. 17 Schematic of electro spinning[74]

2.2.4.5 Yarn-Solution Casting

Recently, there is also reports on preparing of polmer/CNT composites using a continuous solution casting method. Figure 2.18 shows the principle and process of the synthesis method[75].

Here, the continuous super aligned carbon nanotube (SACNT) arrays were s twisted into yarn by a motor then passed throught the PVA solution which were placed on a heating plate. After being covered by PVA solution, the yarn then went through a tube furance to evaporate the solvent. The composite fiber will collected by a roating collector. Author reported a tensile strength of 1.95 GPa for this fiber. In comparision, the strength of the original twisted SACNT yarn is only 0.54 Gpa.

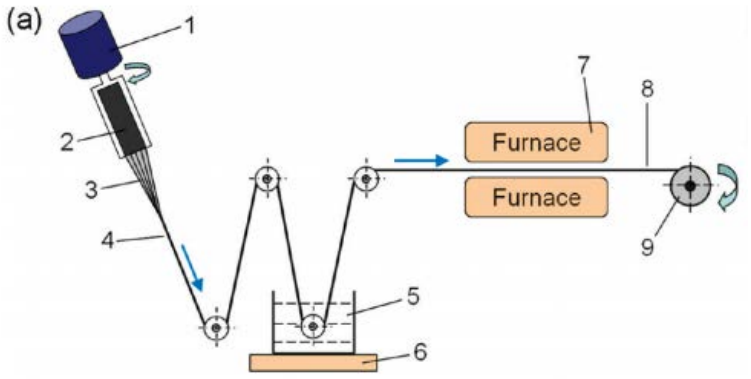

Figure2. 18 Schematic of yarn-solution casting

There are other methods of fabricating polymer nanocomposites, such as to spray polymer solution on the CNT array[76]. In this process, during the drawing of CNT Buckpaper from the array, dilute PVA solution was sprayed on the CNT sheet instead of using solution casting. The tensile sgtrength of composite film synthesized by this method can reach 1.8 Gpa, which is very close to that from solution casting method.

Chapter 3: Sample Fabrication and Characterization Methods

In this section, we discuss the sample synthesis process, experimental setup and characterization techniques used in our study. The reason for choosing the PVA system and processing solvents will be discussed here. Experimental testing methods discussed here include tensile test, dynamic mechanical analysis (DMA), differential scaaning calorimetry (DSC) analysis and scanning electron microscope (SEM) studies. The first three methods are used to characterize mechanical properties and their temperature dependences for the composite material; which also provide information on the interaction between polymer chain and CNFs. SEM is used to characterize the microstructure and morphology of the composite.

3.1 Sample Preparation

3.1.1 PVA and Solvent

Commerically avaliable PVA has different grades based on their degree of hydrolyzation level. Three most common PVA grades eare: 77%-79% hydrolyzed, 87%-89% hydrolyzed and 98%-99% hydrolyzed. The hydrolyzed degree indicates the ratio of remaining ester group on the polymer chain. In this study, we used highly hydrolyzed PVA to achieve ensure the ester group has minimum effect on the structure and property of composite.

Polymerization degree is another factor determining polymer properties. Molecular weight is used to describe the degree of polymerization and it is an evaluation of average length of polymer chains. Commercially available PVA can have following three molecular weight ranges:

Low molecular weight, the average molecular weight ranges from 10000 to 26000;

Medium molecular weight, the average molecular weight ranges from 57,000 to 66,000;

High molecular weight, the average molecular weight ranges from 88,000-97,000.

Figure 3. 1 PVA with different molecular weight

In this study we used low molecular weight PVA due to it is higher solubility. Shorter molecular chain also indicates there can be more interactions between the polymer chain and carbon nanofillers.

3.1.2 Solvent Choice

Due to the high polarity of PVA molecules , they have high solubility in polar solvents. Good solvents for PVA include water, dimethyl sulfoxide (DMSO), phenol etc.

DMSO is a colorless organosulfur liquid and also a aprotic polar solvent. It is a better solvent than water here because its better wetability to CNFs than water. Also it was found that the mixtures of 40% DMSO/water mixture is easy to form gel, so pure

DMSO was used in this study. Figure 3.2 shows the molecular strucutre of DMSO - $(CH_3)_2SO$.

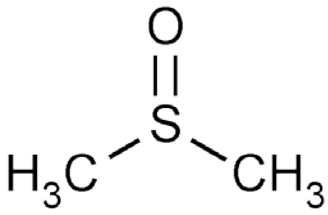

Figure 3. 2 Chemical structure of DMSO

Chemicals used in this research include :

Polyvinyl alcohol (average molecular weight 10000-26000, 98%-99% hydrolyzed, purchased from Alfa Aesar)

DMSO (anhydrous ≥99.9%, purchased from Sigma-Aldrich)

Due to the high degree of hydrolyzation of used PVA, the dissolution process was performed at a temperature around 80-90℃, which was much lower than the boiling point of DMSO. So DMSO evaporation during processing.

3.1.3 Carbon Nanofiber Sheet Synthesis

The carbon nanofibers we used in this study were the PR-24-XT-LHT supplied by Pyrograf Products, Inc. These CNFs are produced by fluidbed CVD process. Average CNF diameter is about100 nm with average length between 50-100 micron and CNF surface area is around 43m^2/g.

Carbon nanofiber sheet was fabricated from carbon nanofibers, using the dispertion and filtration method. Comparing with the traditional way by acid treatment,

the carbon nanofibers here have been soaked into Fento reagent (H_2O_2 and Fe Oxidation System) for at least two hours for the purpose to creat hydroxy groups and carboxy groups to the fiber surface. Surfactants such as SDS, SDBS CTAB were used to further improve CNF dispersion in solvent. After filtration and dry at 100 ℃ with pressure, carbon nanofiber sheets will form. Figure 3.3 show the self-standing carbon nanofiber sheet used in this study.

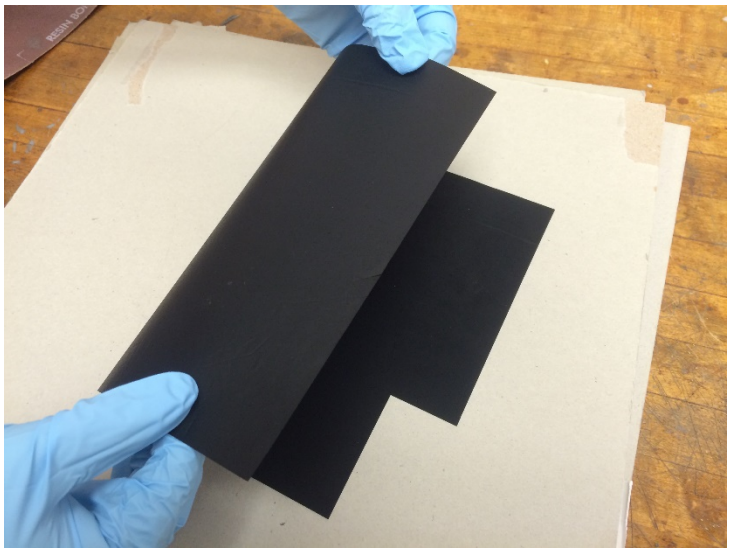

Figure 3. 3 Self-standing carbon nanofiber sheet

3.1.4 PVA-CNF Buckypaper Composite Synthesis

We used solution casting method to prepare our testing samples. Comparing with the traditional way of direct mixing of CNFs with liquid phase polymer to prepare composites , our method here is much simpler and faster, but more importantly, better control of the filler distribution can be achieved.

Here are the typical procedures for our sample preparation.

1. 50 ml DMSO is heated to 90℃ on a heating plate

2. After DMSO temperature is stablized at 90℃, 8.8235g PVA is added to achieve 15% weight precentage. The mixture is kept under magnetic stirring for 3 hours untile all PVA is dissolved. During the entire dissovling process, the mixture temperature should be kept at above 80 ℃
3. Turn off the heating and after the solution cools down to room temperature, put the sloution in vacuum to degas.

Figure 3. 4 PVA/CNFs sheet composite preparation

4. Repeat the degas step for 3-4 times until no bubbles can be observed in solution .
5. Cut the carbon nanofiber sheet into small strips with dimensions of L:10mm× W:4mm ×thickness: 90μm, and wet the CNF strips by DMSO.
6. Place wetted CNF stripes into the petridish and organize them in pattern and using pipette to add 27 ml 15% wt PVA/DMSO solution into this petri dish. Meanwhile, prepare pure PVA reference samples under the same procedure.

7. After the PVA/DMSO solution interact with CNF strips, degas the samples again to remove air in the CNF.
8. Put petri dishes into vacuum oven and heat the samples to 40℃ with and keep the vacuum pressure at -14 psi to facilitate the solvent evaporation
9. Keep on checking sample weight and cut out samples for characterization.

3.2 Characterization methods

3.2.1 Dynamic Mechanical Testing and Analysis

The dynamical mehchanical behavior of the composite samples was measured using DMA. During the measurement an alternating strain is applied with corresponding time dependent stress recorded. DMA measurements provide information on the polymer viscoelasticity which reflects the the polymer chain structure and their movement under stress.

If a stress in the sinusoidal form applied to a sample, due to different materials properties, the strain response of different materials can be very different. For example, when the applied stress is in the form of

$$\sigma(t) = \hat{\sigma} sin\omega t \tag{3.1}$$

$\hat{\sigma}$ is the peak value of stress $\sigma(t)$

ω is angular frequency

t is time

For ideal elastic solid, the strain response can be expressed as

$$\varepsilon(t) = \hat{\varepsilon} sin\omega t \tag{3.2}$$

$\hat{\varepsilon}$ is the peak value of strain ε.

There is no phase difference between stress and strain, which also means that the work done by external force will not be dissipated by the material. Work and elastic energy stored in the sample can be converted without loss.

The other limit is for ideal viscous liquids, there will be a 90° phase difference between stress and strain, so the strain response can be expressed as

$$\varepsilon(t) = \hat{\varepsilon} sin\left(\omega t - \frac{\pi}{2}\right). \quad (3.3)$$

Since the ideal liquid can not sustain elastic deformation, so all the external work will be dissipated as heat by the liquid.

Polymers, will have both elastic and viscous responses to external stress, this called the viscoelasticity. This viscoelasticity reflected by a phase difference between stress and strain,which in form is

$$\varepsilon(t) = \hat{\varepsilon} \sin(\omega t - \delta). \quad (3.4)$$

Similarly, of applied strain has a form of $\varepsilon(t) = \hat{\varepsilon} sin\omega t$, the corresponding stress will be $\sigma(t) = \hat{\sigma} sin(\omega t + \delta)$, and this time dependent stress can be rewritten as

$$\sigma(t) = \hat{\sigma} sin\omega t cos\delta + \hat{\sigma} cos\omega t sin\delta. \quad (3.5)$$

Now the stress can be treat as having two following parts:

1. The stress has the phase with strain: $\hat{\sigma} sin\omega t cos\delta$ and
2. The stress has a 90° phase difference with strain: $\hat{\sigma} cos\omega t sin\delta$

   When we use modulus E to describe the corelation between stress and strain, the modulus have two parts which can be defined as

$$\mathrm{E}' = \frac{\hat{\sigma} cos\delta}{\hat{\varepsilon}} \text{ and} \tag{3.6}$$

$$\mathrm{E}'' = \frac{\hat{\sigma} sin\delta}{\hat{\varepsilon}}. \tag{3.7}$$

And the stress-strain corelation can be writed as

$$\sigma(\mathrm{t}) = \mathrm{E}'\hat{\varepsilon} sin\omega t + E''\hat{\varepsilon} cos\omega t. \tag{3.8}$$

To charaterized this viscoelastic behavior, we can use the complex modulus:

$$E^* = E' + iE'', \tag{3.9}$$

where E' is the storage modulus, and E'' is the loss modulus. A loss angle tangent can also be defined by $\tan\delta = \frac{E''}{E'}$. (3.10)

Polymers normally show strong temperature dependent structrural and properties transition around the room temperature. So they will show very different dynamical behaviors when temperature changes. The movement of polymer chains are under significant constrains when temeprature is below glass transition temperture T_g. Above this temperature, polymers will enter a rubbery plateau region where polymer chains begin to move but under high frictional resistance. With increasing temperature, the polymer viscocity will continue to drop. So normally the loss modulus of glassy state polymer is relative low and there is increasing frictional resistance when temperature increases and at even higher temperature it can drop again with decreasing material viscosity.

DMA allows us to measure the measuring storage modulus, loss modulus and loss angle tangent as a function of sample temperature.

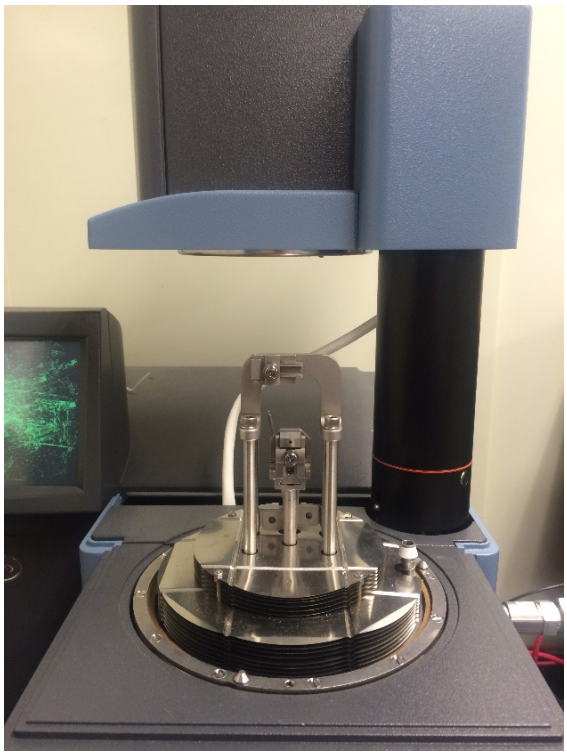

Figure 3. 5 DMA Q800 and tensile sample clamp

In our experiment a TA DMA Q800 was used. The instrument was operated under a tension mode with the sample being placed between a fixed and a moveable clamps. The sample was strain controlled with the reciprocating motion of moveable clamp under preset frequency.

For the dynamical test, we used the DMA Multi frequency-strain test mode and choose the Temperature Ramp/Frequency Sweep test. With known sample dimension and given frequency, the storage modulus, loss modulus and loss angle tangent measurements as a function of temperature can be measured.

PVA will degrade at high temperature and for this experiment, the maximum temperature for the dynamical test was set at 170℃ to prevent. Samples were pre-heated to 65 ℃ in nitrogen environment to eliminate thermal history effects. We chose

appropriate cooling/heating rates to ensure thermal equilibrium can be reached during measurements. Results obtained with a 2℃/min heating/cooling rate and a strain frequency of 1Hz are presented. Nitrogen was used as the protection environment.

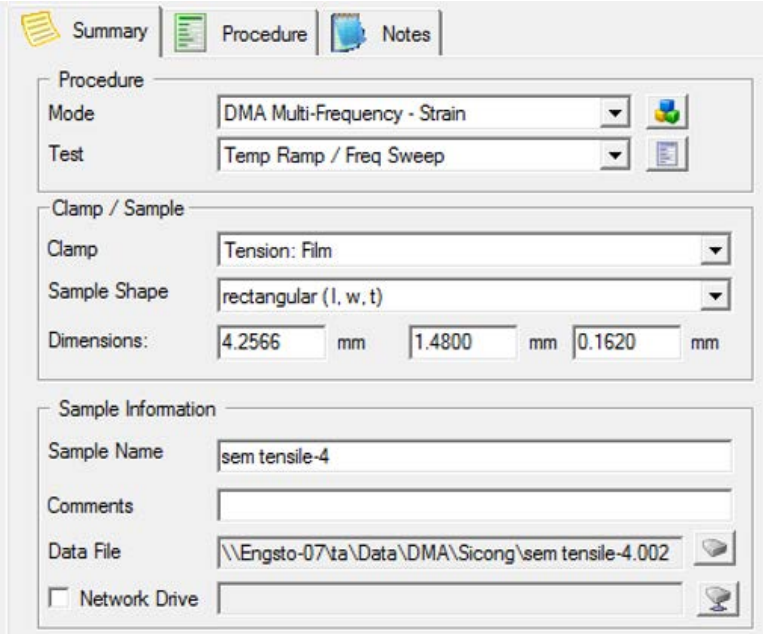

Figure 3. 6 Model set up for DMA test

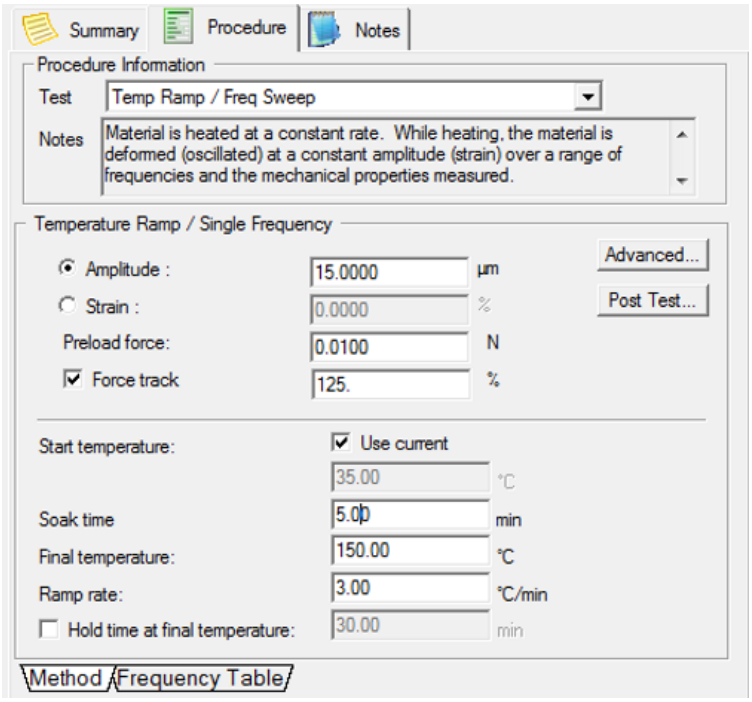

Figure 3. 7 Procedure set up for DMA test

3.2.2 Tensile Test

Static composite mechanical properties are characterized by tensile test through stress-strain measurement.

DMA Q800 also has the capability of performing the static measurement. Here we used the Controlled Force/Strain Rate mode for the static mechanical test. Tests were performed on samples with the same dimension as the dynamic measurments to ensure the consistency of the experiment. A pre-added force of 0.001N is used to keep the sample stay in straight state without bending .

The applied engineering stress and corresponding engineering strain are calculated by

$$\sigma = \frac{F}{A}, \tag{3.11}$$

where F is the applied force;

A is the cross section area.

The definition of strain is

$$\delta = \frac{\Delta l}{l_0} \tag{3.12}$$

Δl is the change of length when load applied

$l_0$is the initial length

When performing DMA static mechanical measurement, we used the force controlled mode. The maximum applied force is 18N and the force ramping speed is 3N/min. The area of cross section was calculated following the volume constant principle.

3.2.3 Differential Scanning Calorimetry (DSC) Analysis

Differential Scanning Calorimetry (DSC) is used to measure sample thermal properties. It measures the heat different between a sample and an reference when changing their temperature. There are two major types of DSCs: the Heat Flux DSC and the Power Compensated DSC. For the Power Compensated DSC, the energy is applied or removed from the sample to ensure the system stay in equilibrium when exothermic or endothermic change happened in the sample. For Heat Flux DSC, temperature difference Δt between the sample and reference is measured continuously as a function of time when they are under the same heating/cooling rate. Then the enthalpy change in sample can be calculated by $\Delta H = \Delta t \cdot R$. where R is the thermal inpedance. R also reflects the sensitivvity of a DSC device.

DSC results are normlly plotted as a curve of heat flux versus temperature or time. The exothermic or endothermic processes are shown as the positive or negative peak, respectively. The enthalpy change during the process also can be calculated by

$$\Delta H = KA, \tag{3.13}$$

where K is the calorimetric constant and A is the area under the curve peak.

DSC curve can be used to determine polymer glass transition temperature (Tg), crystallization temperature (Tc) and melting temperature (Tm). During the heating/cooling process, polymer will under the glassy transition, which is a transition between the glassy state and rubbery state. Upon heating, polymer chain will defrost and become mobil, the specific heat capacity and free volume of polymer will also have a dramatic growth. This phenomenon will be reflected on the DSC curve as a increased heat flow plateau. On the other hand, polymer crystallization is an exothermic process, so

there will also be a correspondent peak on the DSC curve. Correspondingly, their exist a endothermic peak on the DSC curve when polymer melts. The DSC curves will not only be affected by the sample condition but also by the experimentation parameters. Major affecting factors are:

1. Heating/cooling rate of the DSC. The Higher the heating rate, the more prominent of the transition peaks .
2. The residual water or solvent. Water or othe solvent will affect the the movement of polymer chains, and cause a decrease in measured T_g than the actual polymer melting point.
3. Thermal history. Samples experience different thermal history will have different thermal characteristics. To minimize this effect, the sample need to be annealed at temperatures higher than T_g.

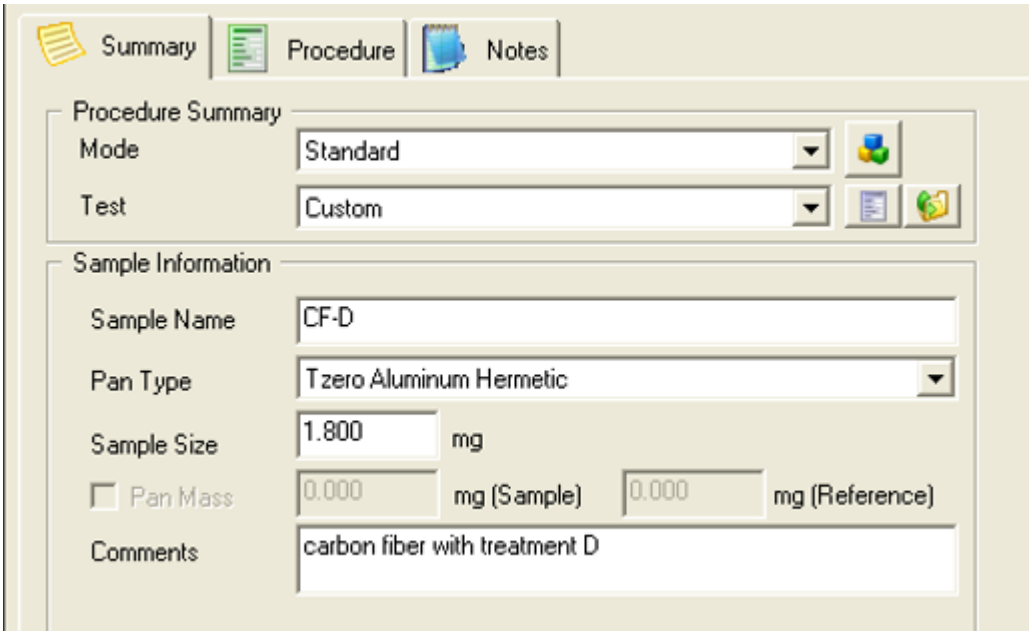

Figure 3. 8 Model set up for DSC test

A TA DSC Q2000 was used in this study. Samples were heated to a temperature above T_g to elinmate the thermal history effect and also residual solvent. Besides, since PVA very sensitive to water, this heating process will also help to reduce water adsoption during test. For the purpose of getting more accurate heat flow/temperature curve with better thermal equilibrium, the heating rate used in the measurement was fixed at $10℃/\mathrm{min}$. The measurement temperature ranges between $150℃$ and $-40℃$ to avoid the PVA crystallization. Heating/cooling cycles were added to observe the repeatability of DSC measurements. In the tests, samples and reference materials were sealed in separate aluminum and hermetic pans. The tests were operated at nitrogen environment and the temperature controled by heating coil and flow of liquid nitrogen, as same as the DMA. Figure 3.8 shows the typical DSC software interface. By customizing the heating/cooling cycles naumbers and specific parameter, we can directly get the heat flow/temperature curves from the device.

Chapter 4 Result and Discussion

This section focuses on the description of experiment results and we will also discuss the mechanism behind the phenomena and analyze the possible reasons. First we will present SEM micrographs to show the microstructure of the composites. Then we will discuss the static mechanical test results to illustrate the CNF mechanical reinforcement effect. We will then present the thermal and temperature dependnet dynamic mechanical characterization results. Based on these results we will discuss the potential application and further material improvement strategies.

4.1 The morphology

4.1.1 Morphology of carbon nanofiber sheet

The carbon nanofiber sheet here was made by the filtration and press drying process. Size of the as-made CNF paper is 30cm by 30cm. Figure 4.1 shows the low magnification micrographs of one side of the CNF Buckypaper. The square surface pattern comes from the filtrate membrane. The other surface exposed in sloution then the pressing plate is smooth. The carbon nanofiber entangled with each other and the Buckypaper is also holding together by the inter-fiber Van der Waals force.

A higher magnification SEM picture, displayed in Figure 4.2, shows most of the fibers in the Buckypaper having a diameter around 100 nm. There are small amount of “out of range” carbon nanofiebrs with extreme large/small diameters. Besides, some residue from processing and dispersion can also be observed. We also found a few carbon nanofibers have branches and bamboo like structure.

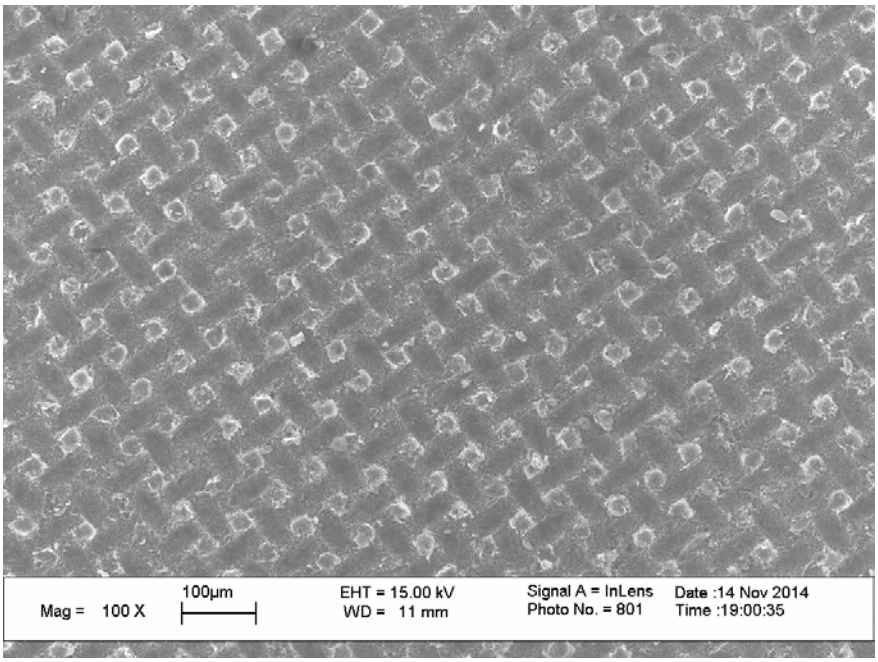

(a)

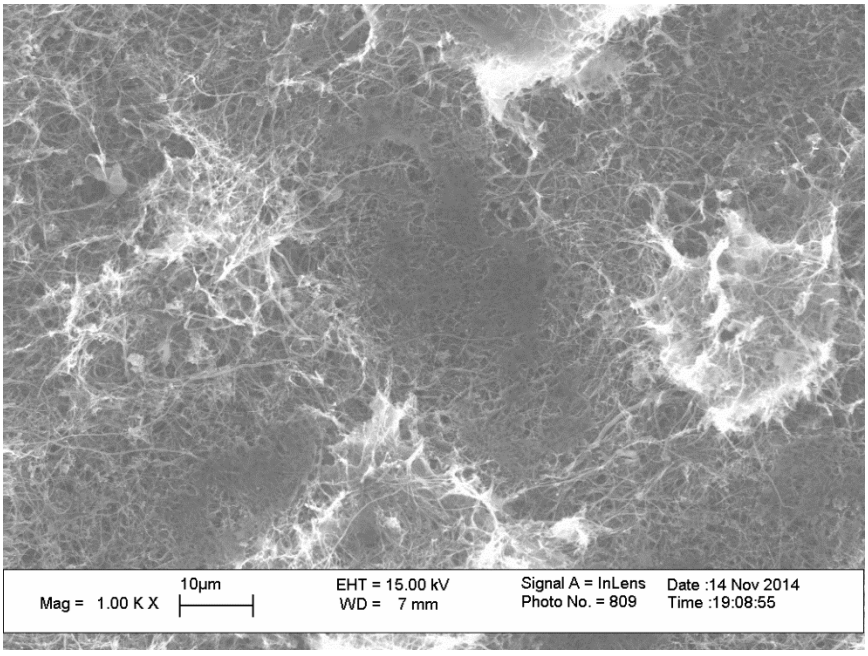

(b)

Figure 4. 1 The SEM micrographs of carbon nanofiber sheet (a) 100X (b) 1000X

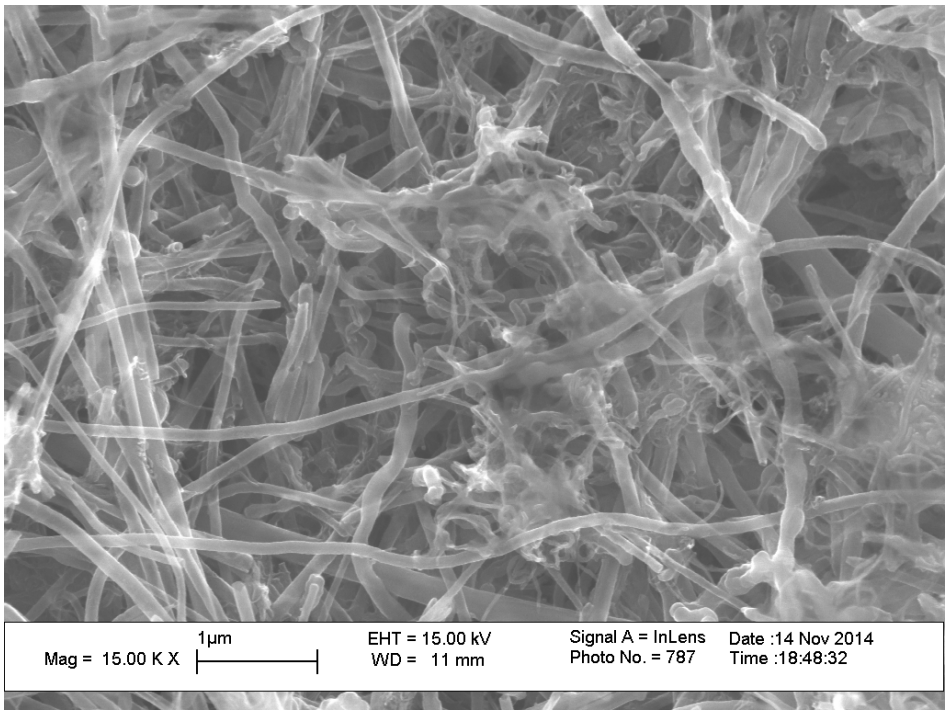

Figure 4. 2 Morphology of CNFs inside the sheet

4.1.2 Morphology of carbon nanofiber sheet PVA composite

Different fabrication approaches will result in different composite morphology and microstructure. Comparing with the direct filler-matrix mixing process, our approach is simpler and only have very limited instrumentation requirement. CNFs paper can be prelaid and made into complicated shapes. In our approach, the polymer needs to be in a low viscosity state, so they can enter the porous Buckypaper structure. So our method could have issues if the ploymer cannnot penetrate the CNF structure. If the CNFs can be appropriately functionalized with other chemical groups, the interfacial interactions betweeen filler and matrix can be enhances and so will the mechanical strength of the composites.

The amount of PVA solution and the choose of solvent will both affect the interactions between matrix and carbon nanofibers. The SEM micrograph shown in Figure 4.3 is the surface of a PVA/CNFs composite sample made with H_2O as solvent.

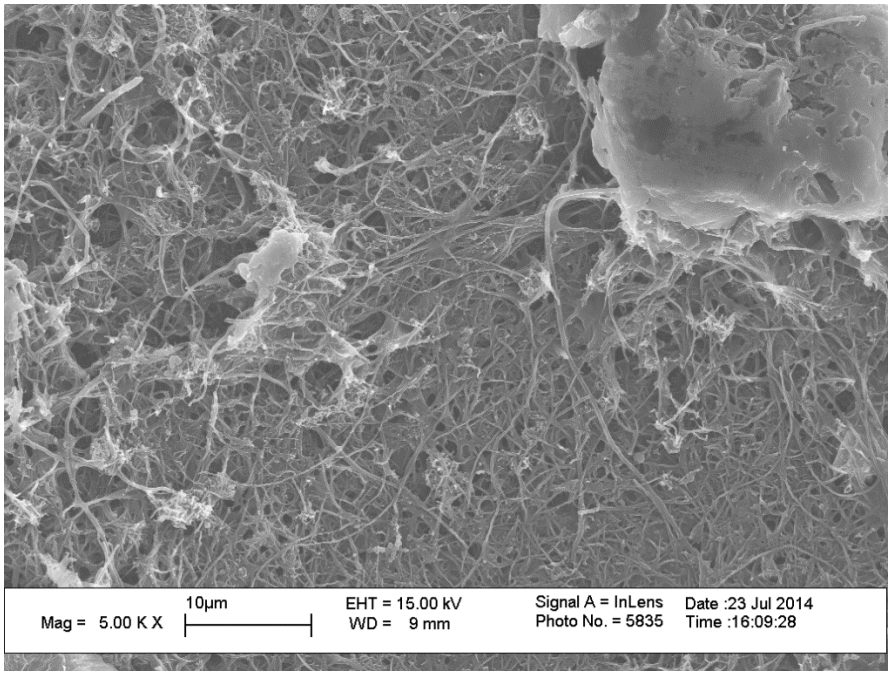

Figure 4. 3 SEM micrograph for PVA/H2O immersed CNFs sheet

We can see from Figure 4.3 that the holes between CNFs are partially full with PVA. Besides that we can see the large bulk parts of PVA still condensated outside the carbon nanofiber sheet after the water evaporation. All these illustrate a bad adhension between PVA/H_2O solution system and carbon nanofibers. CNFs are hydrophobic, during the mixing process, the CNF/H_2O suspension need surfactant such as sodium lauryl sulfate (SDS) for the purpose to wet the CNFs. So when immerse the carbon nano fibe sheet into the PVA/H_2O solution without any surfactant, the soluton will towards to aggregate away from the CNFs.

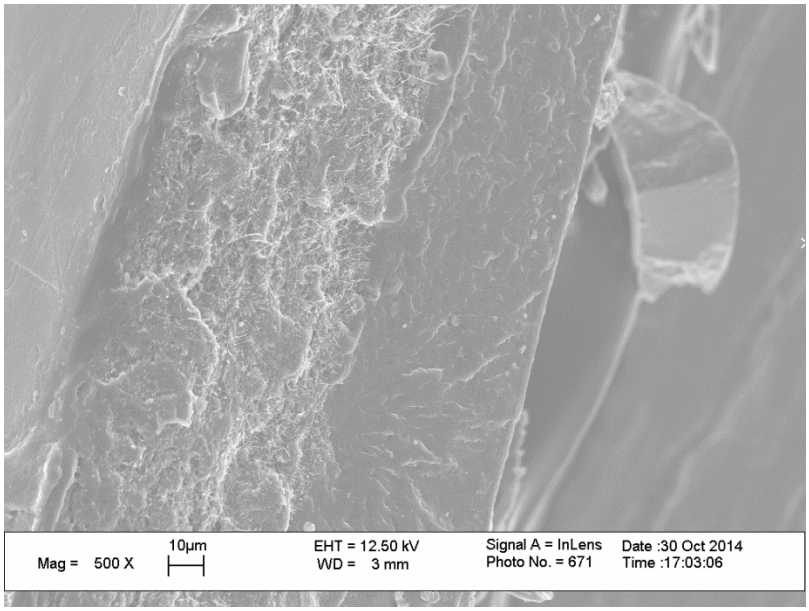

Figure 4. 4 Morphology for fractured cross section of PVA/DMSO immersed

In comparison, Figure 4.4 shows the cross-section of a PVA/Carbon nanofiber composite sample fabricated using the DMSO solvent. A three-layered sandwich structure can be observed with outer pure PVA layers and an inner PVA/CNF Buckypaper composite layer. For DMSO made samples, PVA solution has a better penetration.

Comparing with Figure 4.3, it is clear that the more PVA/DMOS solution penetrate through the carbon nanofiber sheet and, in some term, form a capsulation outside the sheet. Figure 4.5 is schematic of the sample comparation between CNFs sheet-PVA/DMSO system and CHFs sheet-PVA/H_2O system. The top side of sheet in PVA/H_2O can not be totally wetted, but for PVA/DMSO system, the CNFs sheet has been totally penetrated. Figure 4.6 is a high magnification SEM micrograph of the fractured surface taken after tensile test. We can clearly see the hole where the carbon nanofibers have been pull out from the polymer matrix.

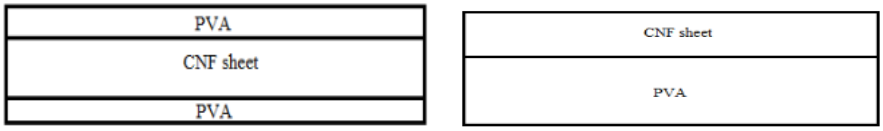

(1) (2)

Figure 4. 5 Schematic of cross section when CNFs sheet immerse into PVA solution: (1) DMSO solution (2) H_2O solution

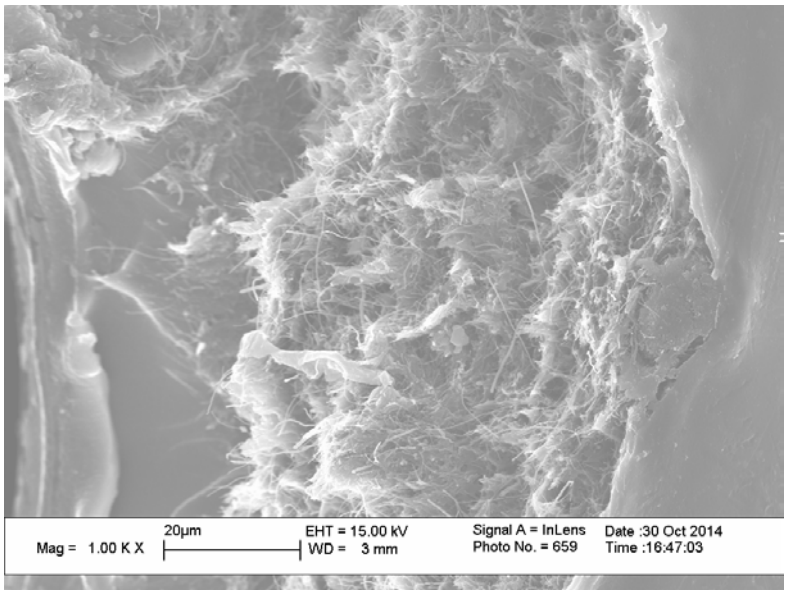

Figure 4. 6 Morphology for fractured cross section.

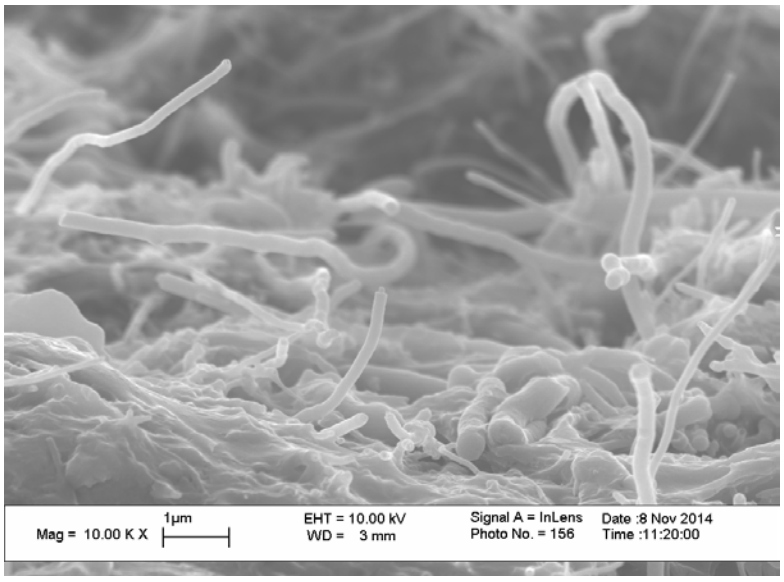

Figure 4. 7 Fibers have been pulled out from PVA matrix

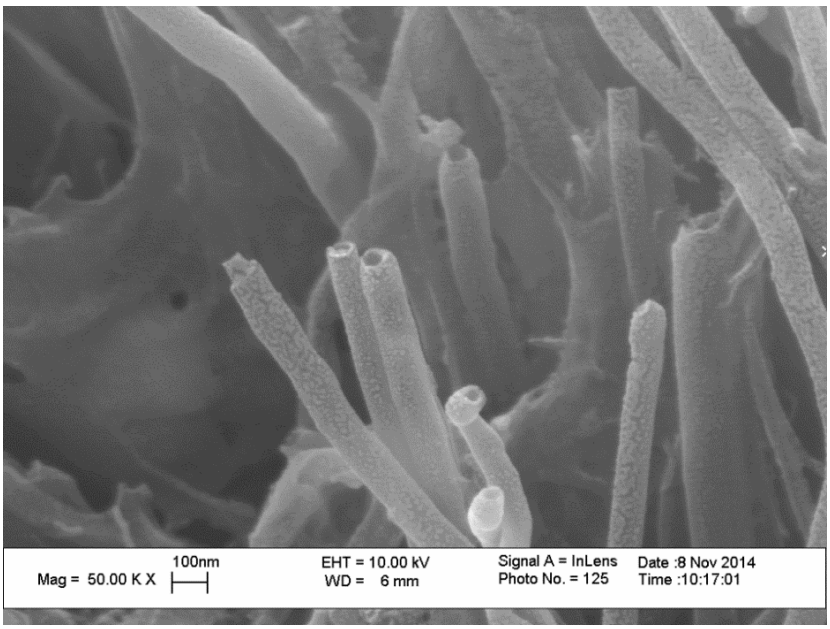

Figure 4. 8 Fiber bundles with shell structure

Figure 4.7 and Figure 4.8 shows a bundle of tubes, We believe these are the PVA shells with pulled-out carbon nanofibers, these PVA shells have different sizes.

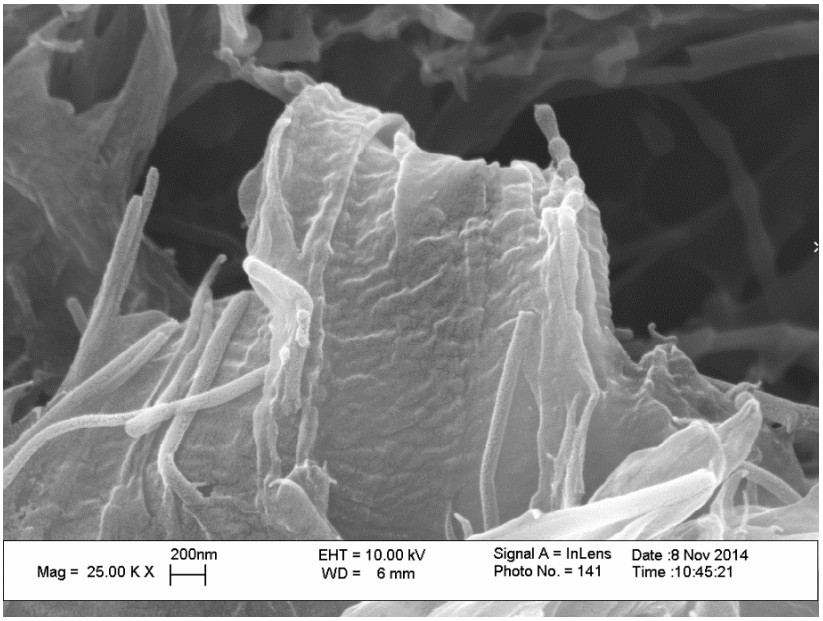

Figure 4. 9 Tube- like interface existed between PVA matrix and CNFs

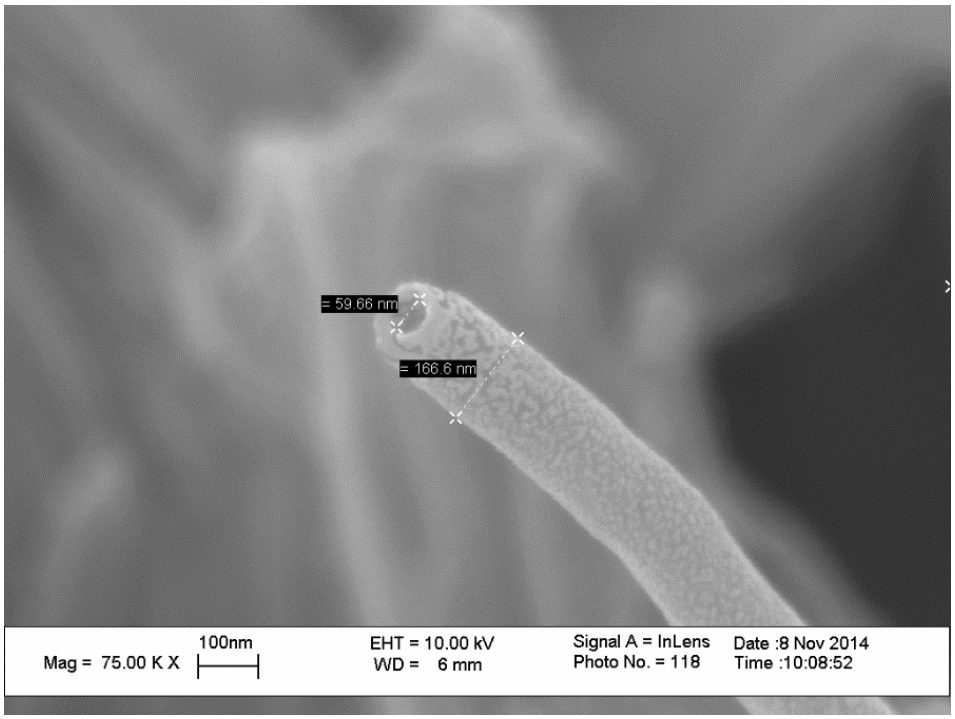
= 59.66 nm
= 166.6 nm
100nm
Mag = 75.00 K X
EHT = 10.00 kV
WD = 6 mm
Signal A = InLens
Photo No. = 118
Date :8 Nov 2014
Time :10:08:52

(a)

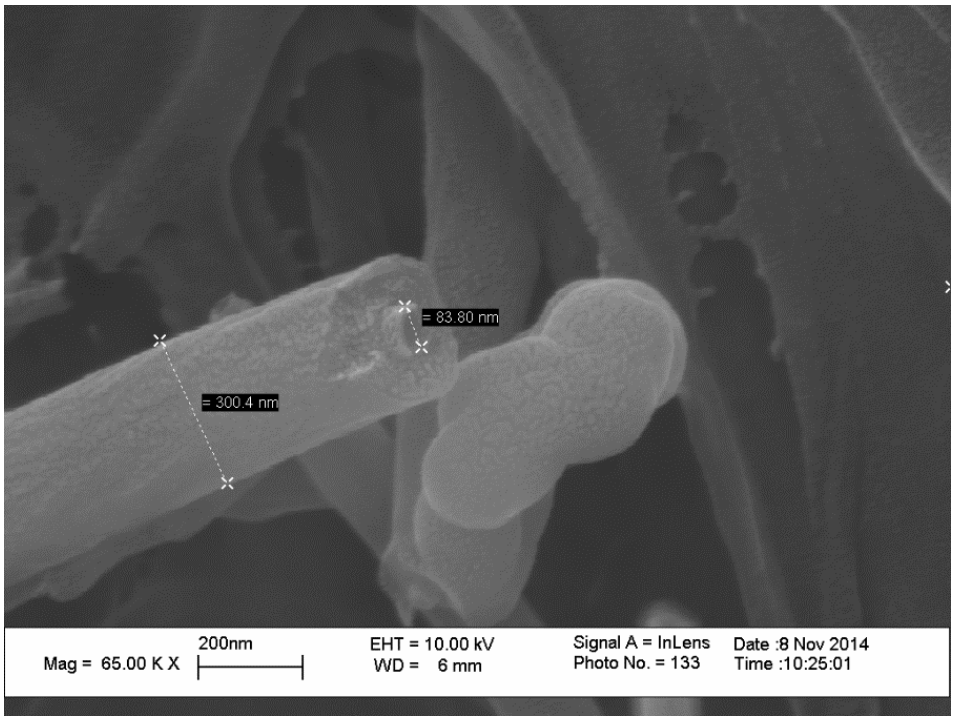
= 83.80 nm
= 300.4 nm
200nm
Mag = 65.00 K X
EHT = 10.00 kV
WD = 6 mm
Signal A = InLens
Photo No. = 133
Date :8 Nov 2014
Time :10:25:01

(b)

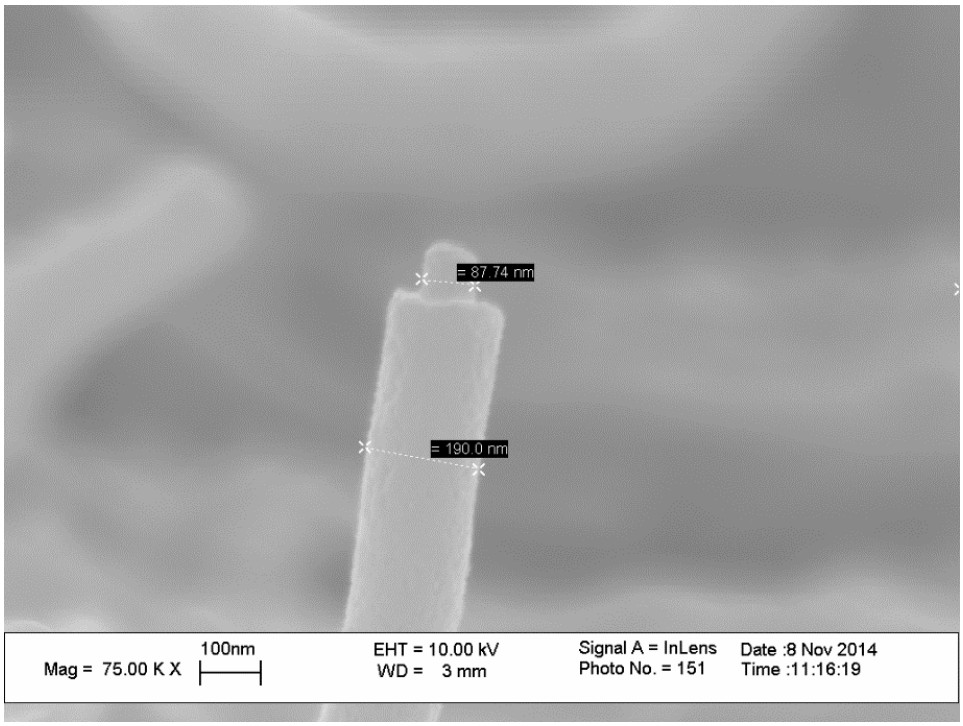

(c)

Figure 4. 10 Diameter of inside hole and outside shell for tube fiber

Figure 4.10 (a) shows a high magnification image of a PVA tube. The outer diameter of the tube is 166.6 nm and the inner diameter is 59.66 nm. Figure 4.10 (b) shows another two parts structure, with a outer diameter of 300.4 nm and an inner of 83.8 nm. In Figure 4.10 (b) , the fractured CNF extrudes out of the the PVA shell. Figure 4.10 (c) showes yet another such structure with a outer diameter of 190 nm and inner structure with a diameter of 87.74 nm.

Arrow shown in Figure 4.11 indicates a PVA layer was stretched after nanofiber fracture and separation. Figure 4.10 here proved that it is PVA shell outside the CNFs. One of the shell has been almost separated from the PVA matrix but still keep a connection between matrix and tube.

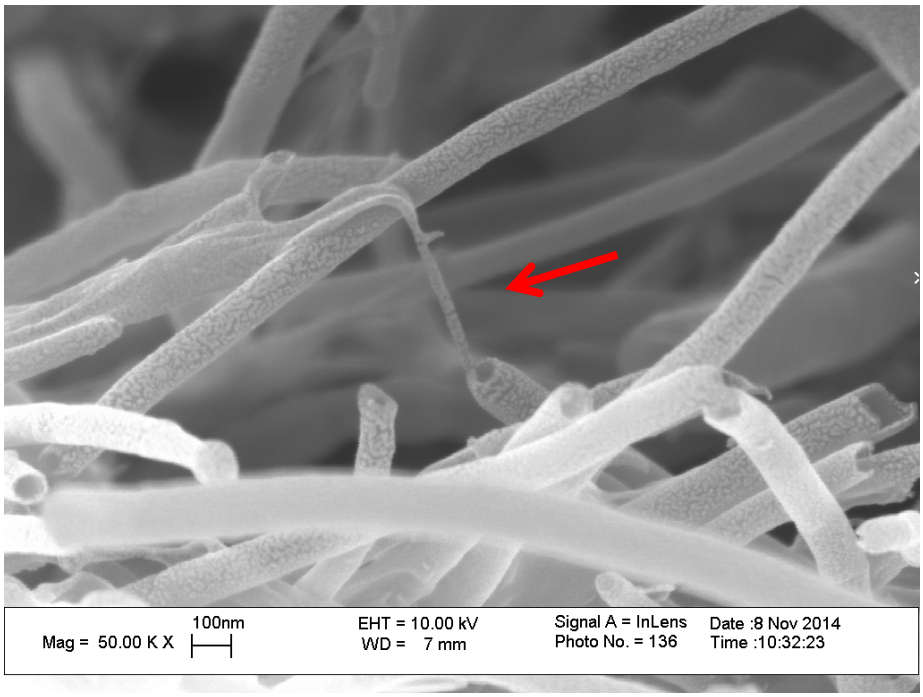

Figure 4. 11 Fracture part of PVA shell

The formation of intermediate polymer layers on the surface of nanofillers has been reported by several groups when studying CNF/CNT nanocomposites. For example, Al-saleh *et al* have oberved that the HDPE covering VGCNF can extend out from the fracture surface. The interfacial polymer layer formed between bulk polymer matrix and carbon fibers can have significant effect on the mechanical property of a composite materials. Their mechanical properties are different from both the fillers and polymer matrix. These PVA layers formed between the CNF and PVA matrix form bondings with both materials. Current observations indicatedthat the CNF/interlayer PVA bondings are stronger than the bonding between the two PVA materials.

The possible reason for forming the middle PVA layer is due to the use of DMSO solvent. As an aprotic polar solvent, DMSO can attract both PVA polymer and CNFs. When the CNFs are immersed into the PVA/DMSO solution, DMSO could easily

permeated into the carbon nanofiber sheet and cover the CNF surface. Their advantage of weeting the CNFs will also introducing PVA chains to moving inside the sheet. During the evaporation process, DMSO has been move out and PVA will stay behind and form a shell like interface outside the CNFs. On the other hand, the high surface tension will shrik the volume of carbon nanofiber sheet which is good for hydrogen bonding formation between functional groups on the CNFs surface and PVA chains.

Figure 4.12 show that there exists debonding between outside PVA layers and PVA/CNFs composite layer on the fracture surface after tensile tested. The reason here could be that the outside coating PVA have large plastic deformation, however, for inner layer with CNF network, more elastic deformation happened during this process. After infiltrated with poylmer, bumps which contain carbon nanofiber could reduce the debonding between two layers. The reason and mechanism will disscussed in static mechanical property part.

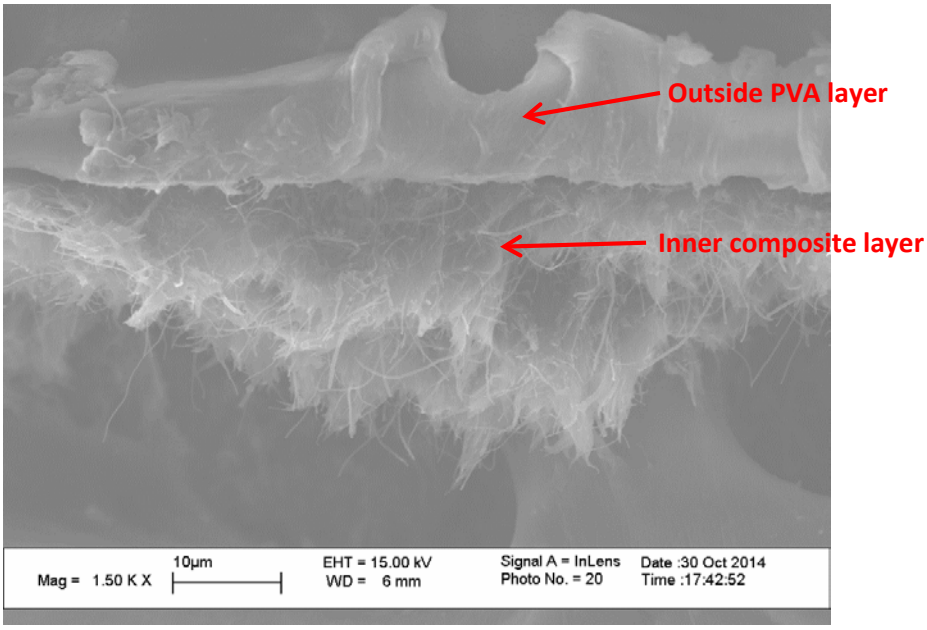

Figure 4. 12 Debonding between outside PVA layers and PVA/CNFs composite layer (top view)

4.2 Static Mechanical Properties

4.2.1 Static mechanical properties of Pure PVA

The tnesile test were performed on PVA soultion casting CNF sheet stripes, and pure PVA with same size. The test operated on DMA Q800 the tensile test model with control force. With proload force 0.001N, the tensile force will increaing to 18N from 0.001N with force ramp rate 3N/min. All the tests operated under nitrogen environment to remove the effect of water and in room temperature.

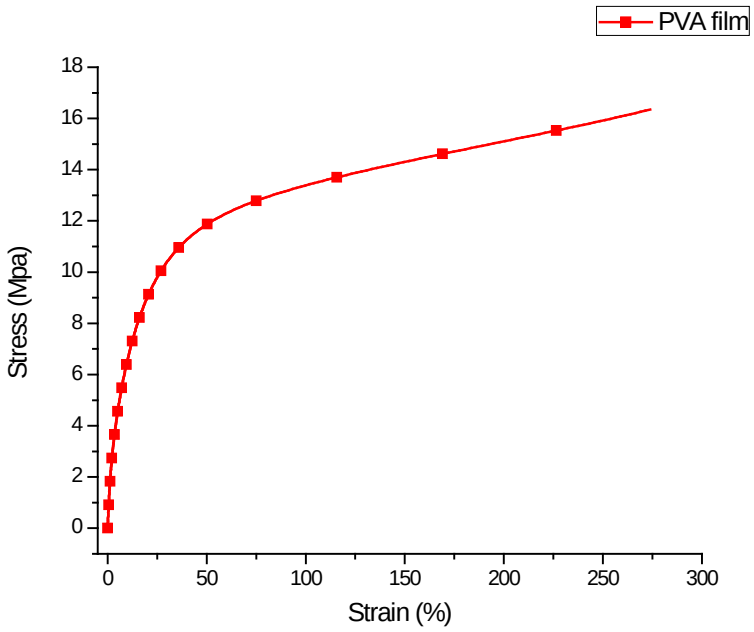

Figure 4. 13 Stress/Strain curve for pure PVA

The typical Stress-Strain curve of pure PVA thin film show by Figure 4.13. This is a typically amorphous state PVA stress-strain curve which under temperature below the T_g. Before the sample reach the yield point, the sample obey Hooke's law, it will totally recover after release the stress and no unrecover deformation. After the yield point, plastic deformation happened and the cross section of sample getting thinner and form a

"neck", with the increase of strss, the width of neck part between two cross heads will getting smaller. The test above T_g illustrate the mobility of polymer is much higher than it in glassy state. In the elastic region, the deformation still limited in random coil chain conformation change. The plastic deformation before yield come from the disentanglement of PVA chains, which mean the chain configuration will convert to more strectchable state. When the chain configuration enlongated at force direction, it is more easily for chains slippage. However, our sample here has not breaked yet due to the limitation of maximum distance between two cross heads. But we still can see that the plastic deformation has already reach 300%. So it is clear that for pure PVA, it is a very soft and ductile polymer mateiral when temperature below T_g. If we increase the temperature highly above T_g during the evaporation and dry process, the PVA will possibly become semi-crystallized and follow another stress-strain curve.

4.2.2 Static mechanical properties of PVA/carbon nanofiber sheet composite

The PVA/CNF sheet composite tested under same condition as pure PVA test. The composite show much different static mechanical behavior than pure PVA. We can see the turning point just appear when the force teach maximum. The maximum strain for these three samples will given by follow table. Comparing with the pure pva samples, the elastic region getting bigger which indicate that the CNFs network can efficiently take the load for polymer matrix. From this table we can see that for the maximum strain we can get when stress reach 18N is about 37.3%. As the blue line indicated in the Figure 4.14, composite sample 3 almost pass the yield point which is weaker than other two, it is could casued by the local nonuniform of PVA distribution. The residue on the CNFs

sheet could also weaken the bonding between carbon nanofiber sheet and PVA outside layer, which could significantly retard the load transfer.

Table 4. 1 Maximum strain for PVA/CNF sheet composite at 18N

	PVA/CNF sheet 1	PVA/CNF sheet 2	PVA/CNF sheet 3
The maximum strain when stress reach 18N	17.11%	27.57%	37.3%

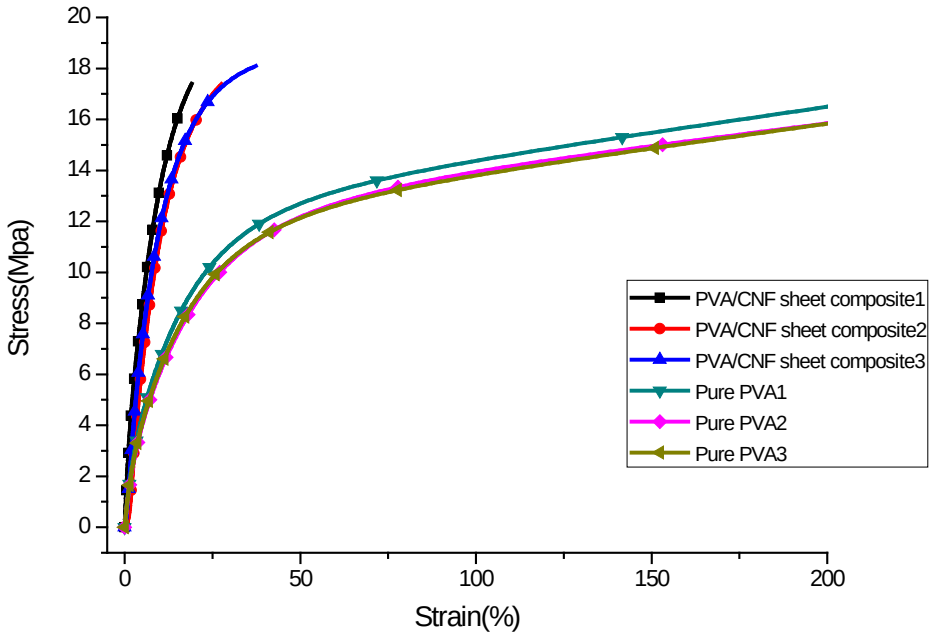

Figure 4. 14 Stress/Strain curve for pure PVA and PVA/CNFs sheet composite

We cannot find any necking happened on any composite samples during the tensile test. Besides, we can see that higher stress level can endured under same strain level as pure PVA, which means more widely application for the high stress situation which can replace the PVA film.

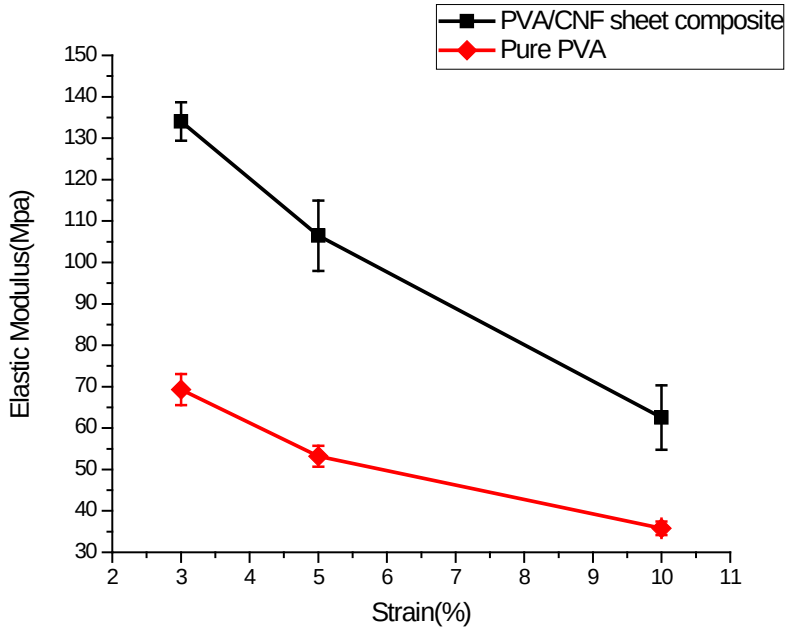

Figure 4. 15 Elastic Modulus at 3%, 5% and 10% strain

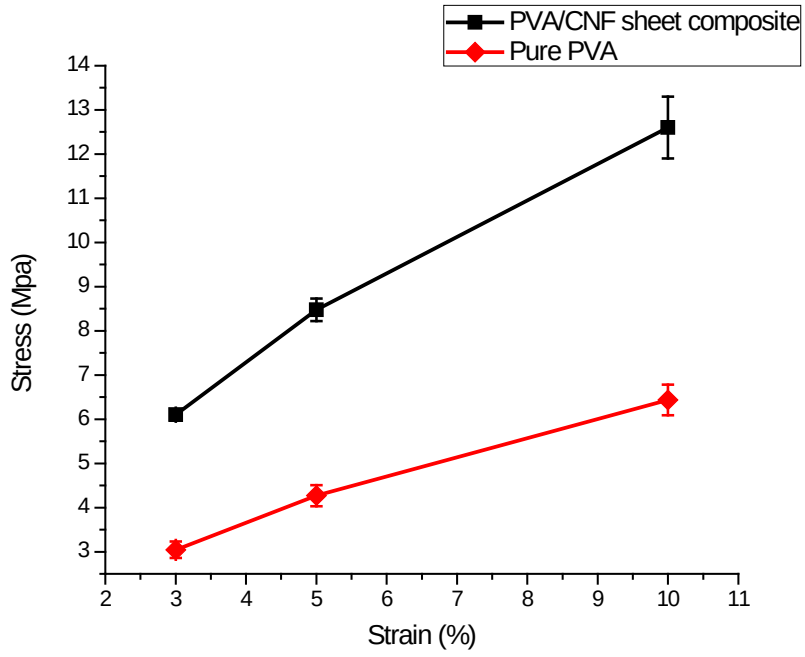

Figure 4. 16 Stress at 3%, 5% and 10%

Figure 4.15 provide the modulus comparsion between pure PVA samples and composite samples. The modulus on 3%, 5% and 10% strain provided here respectively. The sample still in elastic deformation region when strain are 3, 5% and 10%. Here we can see that with 3% strain, the modulus increase from 69.3 Mpa to 134.05 Mpa, which is more than twice of pure PVA. For 5% strain, the modulus increase from 53.19 Mpa to 106.46 Mpa. For 10% strain, the modulus increase from 35.8 Mpa to 62.57 Mpa. These data here show CNFs sheet effectively take the load from the PVA matrix and increase the modulus of composotie. During the tensile test, the configuration of PVA could be more possible stay in their nature position due to the entanglement between chains and fibers and fixed position of CNF. The fixed position CNF will retard the unfold of PVA coil by both physical and chemical methods.(Figure 4.17)

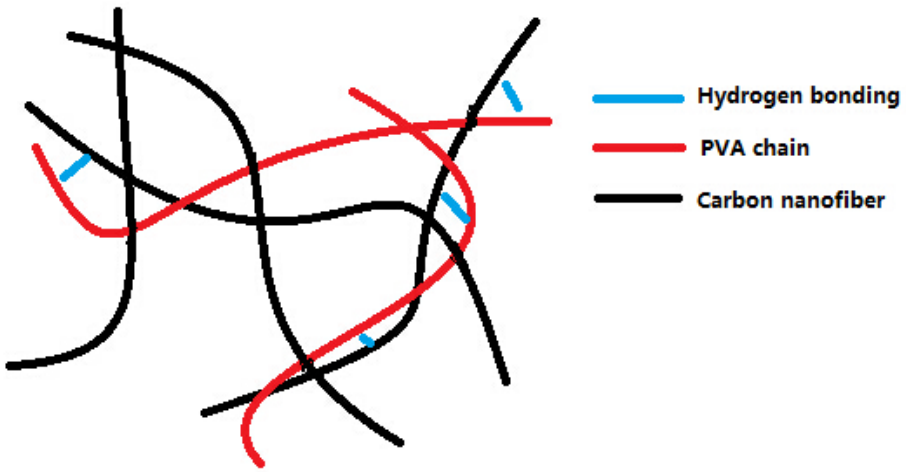

Figure 4. 17 The schematic for physical and chemical entanglement between PVA chains and CNFs

The slightly decreasing in reforced ability possibly result from the pure PVA layer outside of the composite, which also take the load under outside force. It is clear that the pure PVA layer will under plastic deformation early than the composite due to no

reinforcement. So when it combine with composite layer, their low modulus will affecting the modulus of whole sample. The relationship between stress and strain in 3%, 5% and 10% also can prove this point. So the adhension between outside PVA layer and compsite are significant for the static mechanical property of PVA/CNFs sheet composite.

On the other side, for our samples the weight percentage is around 20%, however for the composite layer inside the weight precentage of CNFs is much higher than 20%. It can be treated as the CNF network nested inside the PVA matrix which achieved unifrom distribution by mixing process. So it is vital that control the amount of PVA solution for the purpose to decrease the outside layer thickness and on the other side, provide enough PVA to penetrate the carbon nanofiber sheet. For example, low concentration of PVA in DMSO solvent could provide more free volume for the PVA chain, which will contribute to the filtration process.

4.3 Dynamical mechanical property of pure PVA and PVA/CNFs sheet

The dynamical mechanical property were investigated by DMA Q800. The storage modulus, loss modulus values and tanθ were compared for pure PVA and PVA/CNFs sheet composite as shown in Fig 4.18, Fig 4.19 and Fig 4.20 respectively.

The storage modulus keeps decreasing when temperature rising. When temperature below T_g, the material response for dynamic load come from the motion of polymer bonds. The polymer chain begin to moving when the temperature above T_g. The movement of polymer chains will cause the internal friction increaing, which is indicated by loss modulus. Here we can see that the CNFs can increas the storage modulus by retard the motion of polymer chain inside the matrix, which is more effective when temperature above T_g. However, comparing with pure PVA film, the storage mudulus of

the composite is only slightly increased when comparing with the significantly increase from the composite which made by mixing method. The main reason could come from the structure of CNFs sheet. During the dynamical mechanical test, the sample always under same frequency stretch and recover process and keep stay in the elastic region, which indicate the load transfer will be homogeneous. The inner layer of PVA/CNFs sheet network decrease the contact area between PVA and CNFs due to that most CNFs will entangled with each other and, limitied by their size, close to each other. This could weake the ability of CNFs to block the motion of PVA chain.

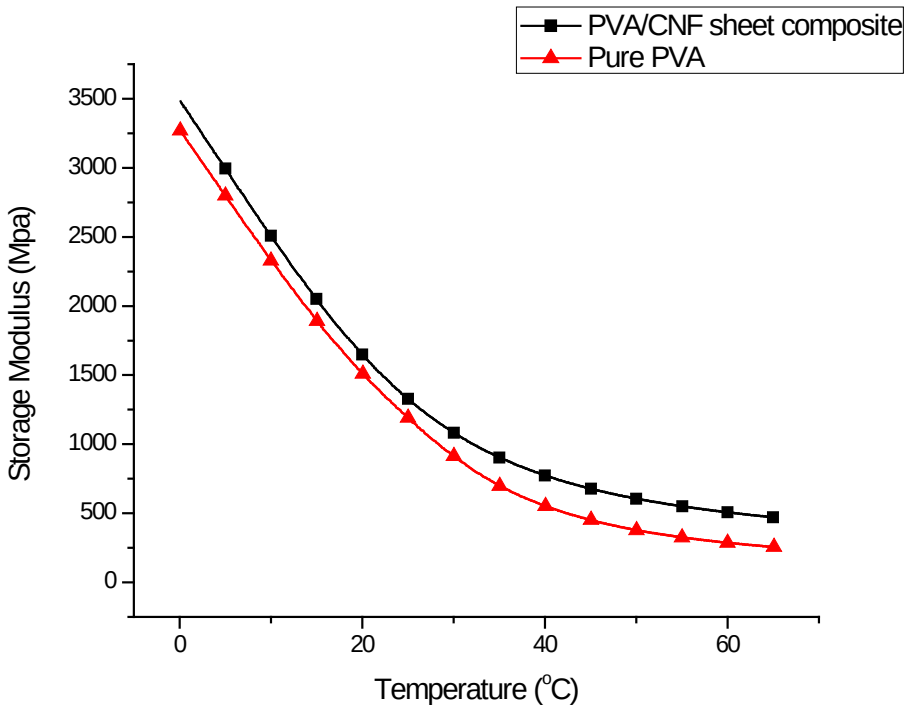

Figure 4. 18 Storage modulus comparison

The loss modulus can reflect the damping property of material. The internal friction can get from the Figure 4.19 which is around 0℃. At this peak, the glass transition happened which indicate the polymer chain begin to move but highest internal

friction appearance due to the high viscosity of the system. Corresponding to the higher storage modulus of CNFs sheet composite, the loss modulus is smaller than the pure PVA. Tangent Delta curve (Figure 4.20) reflect the relationship between storage modulus and loss modulus. The peak of the curve indicate the T_g is around 18.5℃ for pure PVA, at this point, the Tangent Delta has maximum value which indicate the E''/E' has maximum value here. The curve of CNFs sheet compsite show lower value than the pure PVA curve. It is corrosepnding to the increase in storage modulus and decrease in loss modulus. The maximum point of this curve which indicate the T_g, is also not changed. But the present of outside pure PVA layer which encapsulate the carbon nanofiber sheet composite could widen the temperature range for glass transition, which corresponding to broader tangent delta peak in Figure 4.20.

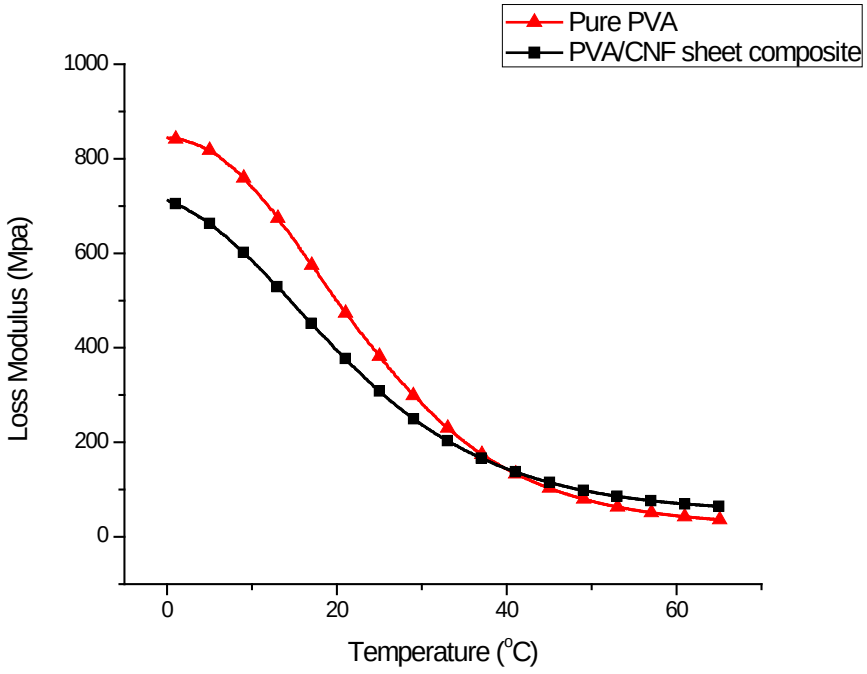

Figure 4. 19 Loss modulus comparison

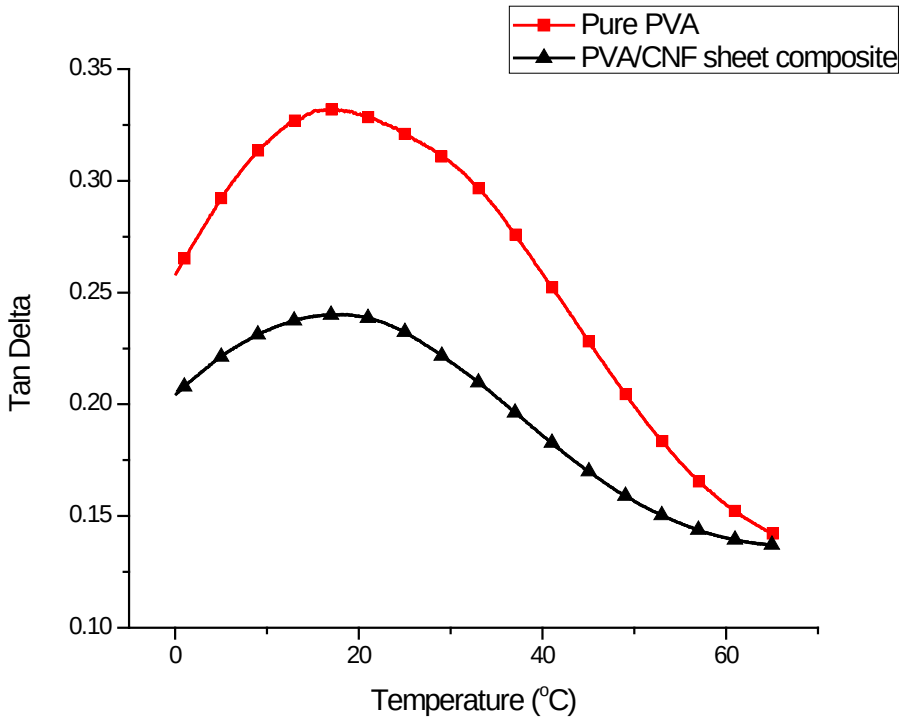

Figure 4. 20 Tangent delta comparison

From the result of dynamical test, we can clear see that the present of CNFs sheet improve the storage modulus of composite by retard the polymer chain movement. The loss modulus, on the other side, is decreaed by the entanglment effect of CNFs sheet.

4.4 Glass Transition Temperature (T_g) Analysis

The T_g measurement operated on DSC Q2000. The detail procedures have been discussed in the experiment section. The sample will pre-heated to 150℃ for the purpose to remove the residual solvent and eliminating the thermal history. The experiment will run two heating/cooling cycles, and the curve during the cooling process will used to measure the T_g for the purpose to vertificate the result from DMA test. Figure 4.21 show the Heat flow/Temperature curve for all cycles of pure PVA.

We can see that the the temperature increasing process for first cycle and second cycle have different heat flow curve, the difference between two curves attributed to the water or solvent inside the polymer and aluminum pan. So it is necessary to do two cycles to check the repeatabiltiy for the heat flow curve. After heating to 150℃, the sample will keep isothermal for 5 minutes to ensure the thermal equilibrium of the sample. The cooling cycles of pure PVA and composite will compared in following figures. The T_g measured by universal analysis software, TA company.

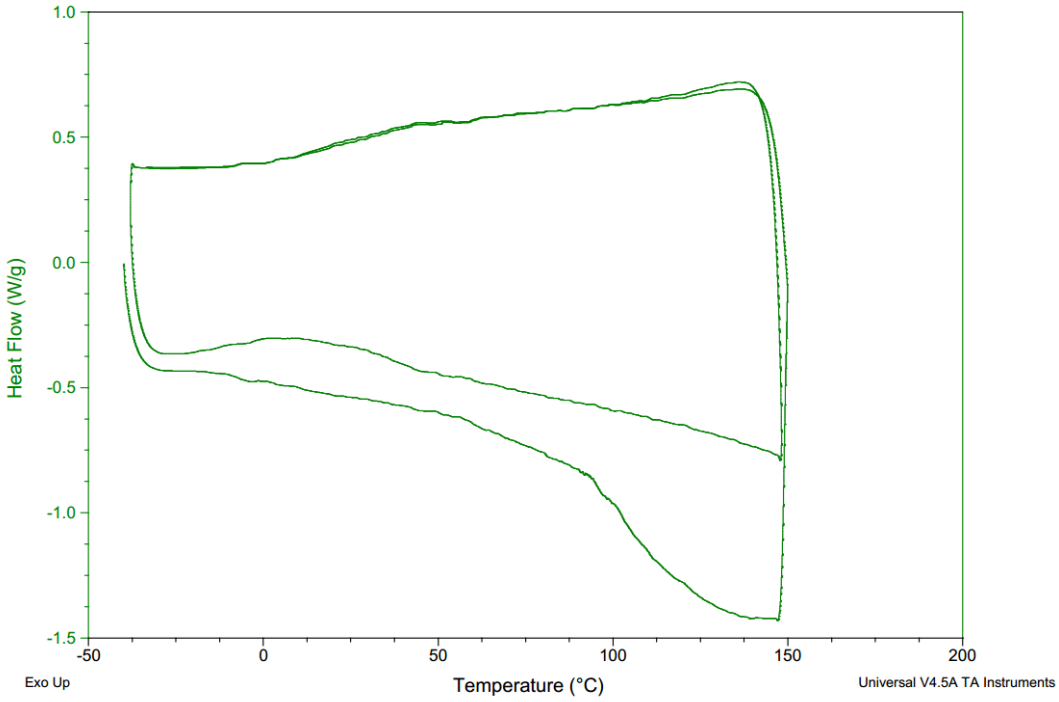

Figure 4. 21 Two cycles of DSC curve for pure pva

From Figure 4.21 and 4.23 it is easy to find the there exist good repeatability between two cycles for PVA and composite. It is easily to find out there exist a transition curver between two heat flow plateaus which indicate the glassy transition zone of PVA and composite. Table 4.2 provide the T_g of pure PVA samlps and PVA/CNFs sheet

composite. The peak for DMA tangent delta curve is 18.5℃. It is obviously T_g measured by DSC confirmed with the data from DMA, and a little increase of T_g were observed on composite samples.

Table 4. 2 Glass transition temperature of PVA and PVA/CNFs composite at different cycles

	Cycle1	Cycle2
Pure PVA	19.04℃	19.06℃
PVA/CNFs sheet composite	21.6℃	22.3℃

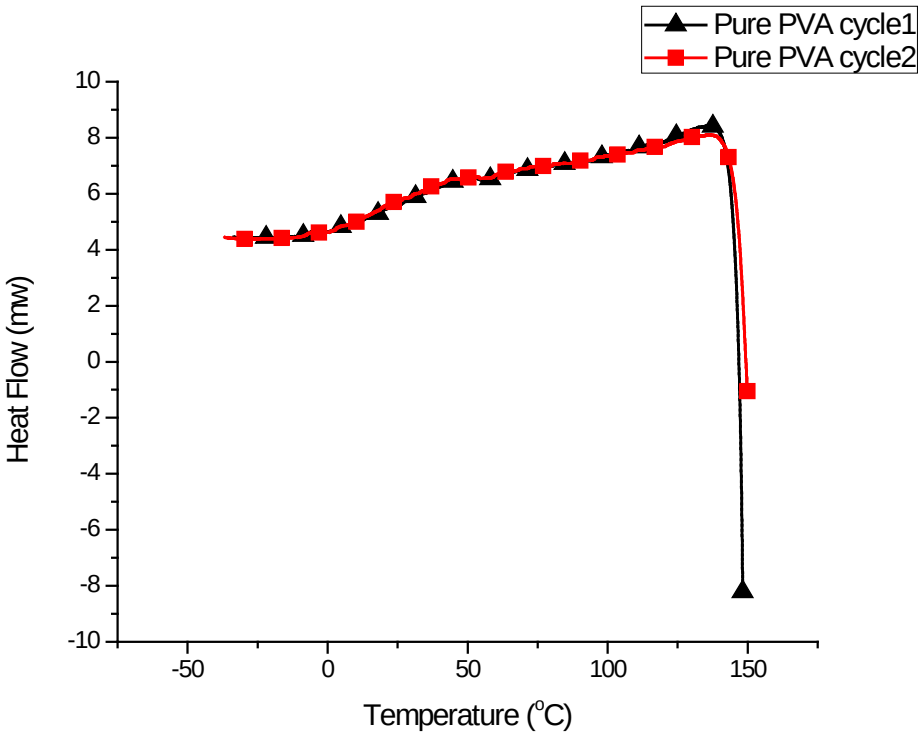

Figure 4. 22 DSC curve for pure PVA cycle 1 and cycle 2 cooling process

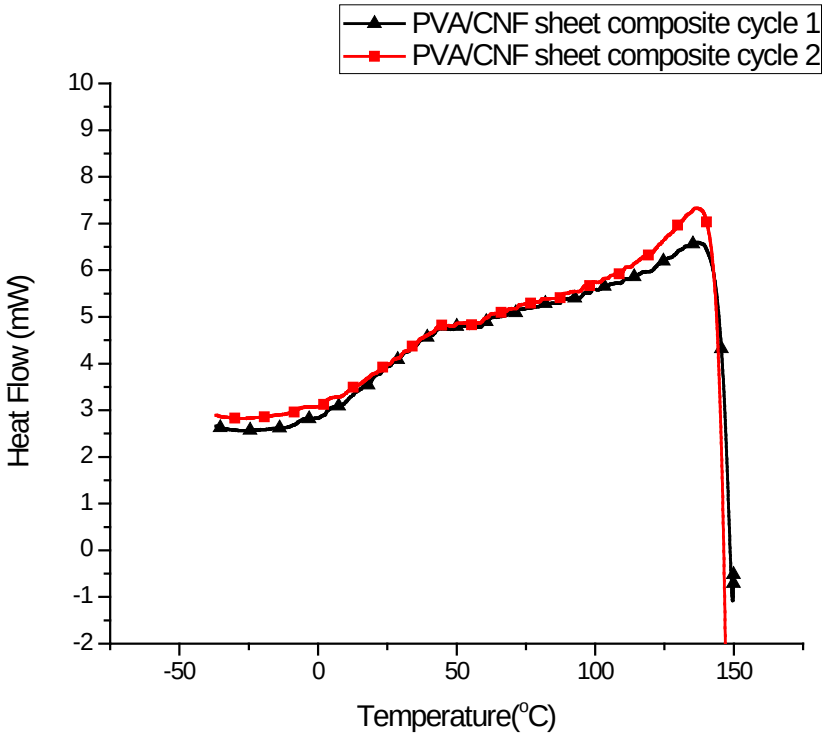

Figure 4. 23 DSC curve for PVA/CNFs sheet composite cycle 1 and cycle 2 cooling process

Chapter 5: Conclusions

Using the self-standing carbon nanofiber sheet as a nanofilling structure, we were able to develop a fast, reproduceble and economical way to fabricate polymer nanocomposites. Our method overcomes the disadvantages of converntional composite synthesis techniques such as solution casting, direct mixing or in-situ polymerization and achieved controlled nanofiller dispersion and makes continuous industrialized manufacting is possible. To improve CNF dispersion, structure uniformity and introduce surface functionaliztion groups, carbon nanofibers have been pretreated with Fento reagent and then make into buckypapers using the wet filtration process.

The chemical adhesion between CNFs and PVA chains have been enhanced by adding surface functionalized groups on CNFs surface to form more interface hydrogen and chemical bondings. The use of aprotic polar solvent DMSO helps PVA to wet the CNF buckypaper. In addition, the DMSO also helps to form a middle layer between the bulk polymer and CNFs, which also further improve the mechanical property of the composite samples.

Due to the limited thickness of CNF Buckypaper and fabrication method. Our samples has a sandwich structure which includes two pure PVA surface layers and a middle compsite layer. The outsice PVA layer is weeker than the middle layer so the actual composite properties can be even better than what is measured. Here doubled modulus and strength have been measured from static mechanical characterization. Now we are optimizing our synthesis method to to decrease the outside layer thickness and further improve adhesion between two layers.

The dynamical mechanical property of composite show higher storage modulus and lower loss modulus. The peak of tangent delta indicates that the T_g has not changed for the composite and its position height is lower and width is wider than those of pure PVA peak. This can be attributed to the outside layer PVA.

DSC measurement also confirmed that the T_g of composite remains close to the pure PVA and is consistant with the DMA measurement. The T_g which measured by heat flow change over time indicate the same result as DMA test of T_g, and the coincidence between two two cooling curves in two cycles respectively confirm the chemical stability of PVA when using as composite matrix.

References

1. Gibson, R. F. (2011). Principles of Composite Material Mechanics, CRC Press.

2. Gogotsi, Y. (2006). Nanomaterials Handbook, CRC press.

3. Çeçen, F. and Ö. Aktas (2011). Activated Carbon for Water and Wastewater Treatment: Integration of Adsorption and Biological Treatment, John Wiley & Sons.

4. Diefendorf, R. and E. Tokarsky (1975). "High Performance Carbon Fibers." Polymer Engineering & Science 15(3): 150-159.

5. Iijima, S. (1991). "Helical microtubules of graphitic carbon." Nature 354(6348): 56-58.

6. Iijima, S. and T. Ichihashi (1993). "Single-shell carbon nanotubes of 1-nm diameter."

7. Bethune, D., C. Klang, M. De Vries, G. Gorman, R. Savoy, J. Vazquez and R. Beyers (1993). "Cobalt-catalysed growth of carbon nanotubes with single-atomic-layer walls."

8. Jose‐Yacaman, M., M. Miki‐Yoshida, L. Rendon and J. Santiesteban (1993). "Catalytic growth of carbon microtubules with fullerene structure." Applied physics letters 62(2): 202-204.

9. Kroto, H. W., A. Allaf and S. Balm (1991). "C60: Buckminsterfullerene." Chemical Reviews 91(6): 1213-1235.

10. Kriitschmer, W., L. D. Lambl, K. Fostiropoulos and D. R. Huffmanl (1990). "Solid C00: a new form of carbon." Geophys. Res. Lett 17(4).

11. Geckeler, K. E. and S. Samal (1999). "Syntheses and properties of macromolecular fullerenes, a review." Polymer International 48(9): 743-757.

12. Hirsch, A. (2010). "The era of carbon allotropes." Nature Materials 9(11): 868-871.

13. Rodriguez, N. M., A. Chambers and R. T. K. Baker (1995). "Catalytic engineering of carbon nanostructures." Langmuir 11(10): 3862-3866.

14. Rodriguez, N. M. (1993). "A review of catalytically grown carbon nanofibers." Journal of Materials Research 8(12): 3233-3250.

15. Al-Saleh, M. H. and U. Sundararaj (2009). "A review of vapor grown carbon nanofiber/polymer conductive composites." Carbon 47(1): 2-22.

16. Endo, M., Y. A. Kim, M. Ezaka, K. Osada, T. Yanagisawa, T. Hayashi, M. Terrones and M. S. Dresselhaus (2003). "Selective and efficient impregnation of metal nanoparticles on cup-stacked-type carbon nanofibers." Nano Letters 3(6): 723-726.

17. Endo, M., Y. Kim, T. Hayashi, K. Nishimura, T. Matusita, K. Miyashita and M. Dresselhaus (2001). "Vapor-grown carbon fibers (VGCFs): basic properties and their battery applications." Carbon 39(9): 1287-1297.

18. Kim, C. and K. Yang (2003). "Electrochemical properties of carbon nanofiber web as an electrode for supercapacitor prepared by electrospinning." Applied Physics Letters 83(6): 1216-1218.

19. Shao, Y., J. Sui, G. Yin and Y. Gao (2008). "Nitrogen-doped carbon nanostructures and their composites as catalytic materials for proton exchange membrane fuel cell." Applied Catalysis B: Environmental 79(1): 89-99.

20. Yang, Y., M. C. Gupta, K. L. Dudley and R. W. Lawrence (2005). "A comparative study of EMI shielding properties of carbon nanofiber and multi-walled carbon nanotube filled polymer composites." Journal of Nanoscience and Nanotechnology 5(6): 927-931.

21. Adhyapak, P., T. Maddanimath, S. Pethkar, A. Chandwadkar, Y. Negi and K. Vijayamohanan (2002). "Application of electrochemically prepared carbon nanofibers in supercapacitors." Journal of Power Sources 109(1): 105-110.

22. Matsumoto, Y., M. Than Oo, M. Nakao, K. Kamimura, Y. Onuma and H. Matsushima (2000). "Preparation of carbon nanofibers by hot filament-assisted sputtering." Materials Science and Engineering: B 74(1): 218-221.

23. Hoshi, F., K. Tsugawa, A. Goto, T. Ishikura, S. Yamashita, M. Yumura, T. Hirao, K. Oura and Y. Koga (2001). "Field emission and structure of aligned carbon

nanofibers deposited by ECR-CVD plasma method." Diamond and Related Materials 10(2): 254-259.

24. Wang, B., S. Lee, H. Yan, B. Hou and S. Choi (2005). "Study on glow discharge effects on catalyst films for growing aligned carbon nanofibers in negative bias-enhanced hot filament chemical vapor deposition system." Thin Solid Films 474(1): 103-108.

25. Che, G., B. Lakshmi, C. Martin, E. Fisher and R. S. Ruoff (1998). "Chemical vapor deposition based synthesis of carbon nanotubes and nanofibers using a template method." Chemistry of Materials 10(1): 260-267.

26. Cheng, J., X. Zhang, F. Liu, J. Tu, H. Lu, Y. Sun and F. Chen (2004). "Long bundles of aligned carbon nanofibers obtained by vertical floating catalyst method." Materials Chemistry and Physics 87(2): 241-245.

27. Ci, L., Y. Li, B. Wei, J. Liang, C. Xu and D. Wu (2000). "Preparation of carbon nanofibers by the floating catalyst method." Carbon 38(14): 1933-1937.

28. Jaeger, H. and T. Behrsing (1994). "The dual nature of vapour-grown carbon fibres." Composites Science and Technology 51(2): 231-242.

29. Ishioka, M., T. Okada and K. Matsubara (1992). "Formation and characteristics of vapor grown carbon fibers prepared in Linz-Donawitz converter gas." Carbon 30(7): 975-979.

30. Chen, X., J. Wang, H. Yang, G. Wu, X. Zhang and W. Li (2001). "Preparation, morphology and microstructure of segmented graphite nanofibers." Diamond and Related Materials **10**(11): 2057-2062.

31. Oberlin, A., M. Endo and T. Koyama (1976). "Filamentous growth of carbon through benzene decomposition." Journal of Crystal Growth 32(3): 335-349.

32. Terrones, M. (2003). "Science and technology of the twenty-first century: synthesis, properties, and applications of carbon nanotubes." Annual Review of Materials Research 33(1): 419-501.

33. Ando, T. (2009). "The electronic properties of graphene and carbon nanotubes." NPG Asia Materials 1(1): 17-21.

34. Daems, N., X. Sheng, I. F. Vankelecom and P. P. Pescarmona (2014). "Metal-free doped carbon materials as electrocatalysts for the oxygen reduction reaction." Journal of Materials Chemistry A 2(12): 4085-4110.

35. Ebbesen, T. and P. Ajayan (1992). "Large-scale synthesis of carbon nanotubes." Nature 358(6383): 220-222.

36. Muhlbauer, R. L. and R. A. Gerhardt "A review on the synthesis of carbon nanotube thin films." Carbon Nanotubes: Synthesis and Properties: 107-156.

37. Ajayan, P., J. Lambert, P. Bernier, L. Barbedette, C. Colliex and J. Planeix (1993). "Growth morphologies during cobalt-catalyzed single-shell carbon nanotube synthesis." Chemical Physics Letters 215(5): 509-517.

38. Huang, H., H. Kajiura, S. Tsutsui, Y. Hirano, M. Miyakoshi, A. Yamada and M. Ata (2001). "Large-scale rooted growth of aligned super bundles of single-walled carbon nanotubes using a directed arc plasma method." Chemical Physics Letters 343(1): 7-14.

39. Ando, Y., X. Zhao, K. Hirahara, K. Suenaga, S. Bandow and S. Iijima (2000). "Mass production of single-wall carbon nanotubes by the arc plasma jet method." Chemical Physics Letters 323(5): 580-585.

40. Journet, C., M. Picher and V. Jourdain (2012). "Carbon nanotube synthesis: from large-scale production to atom-by-atom growth." Nanotechnology 23(14): 142001.

41. Guo, T., P. Nikolaev, A. Thess, D. Colbert and R. Smalley (1995). "Catalytic growth of single-walled manotubes by laser vaporization." Chemical Physics Letters 243(1): 49-54.

42. Thess, A., R. Lee, P. Nikolaev, H. Dai, P. Petit, J. Robert, C. Xu, Y. H. Lee, S. G. Kim and A. G. Rinzler (1996). "Crystalline ropes of metallic carbon nanotubes." Science-AAAS-Weekly Paper Edition 273(5274): 483-487.

43. Chibante, L., A. Thess, J. Alford, M. Diener and R. Smalley (1993). "Solar generation of the fullerenes." The Journal of Physical Chemistry 97(34): 8696-8700.

44. Laplaze, D., P. Bernier, W. Maser, G. Flamant, T. Guillard and A. Loiseau (1998). "Carbon nanotubes: the solar approach." Carbon **36**(5): 685-688.

45. Guillard, T., G. Flamant, J.-F. o. Robert, B. Rivoire, J. Giral and D. Laplaze (2002). "Scale up of a solar reactor for fullerene and nanotube synthesis." Journal of Solar Energy Engineering **124**(1): 22-27.

46. Liu, J., A. G. Rinzler, H. Dai, J. H. Hafner, R. K. Bradley, P. J. Boul, A. Lu, T. Iverson, K. Shelimov and C. B. Huffman (1998). "Fullerene pipes." Science 280(5367): 1253-1256.

47. Whitby, R. L., T. Fukuda, T. Maekawa, S. L. James and S. V. Mikhalovsky (2008). "Geometric control and tuneable pore size distribution of buckypaper and buckydiscs." Carbon 46(6): 949-956.

48. Frackowiak, E., V. Khomenko, K. Jurewicz, K. Lota and F. Beguin (2006). "Supercapacitors based on conducting polymers/nanotubes composites." Journal of Power Sources 153(2): 413-418.

49. Arena, A., N. Donato, G. Saitta, S. Galvagno, C. Milone and A. Pistone (2008). "Photovoltaic properties of multi-walled carbon nanotubes deposited on n-doped silicon." Microelectronics Journal 39(12): 1659-1662.

50. Landi, B. J., M. J. Ganter, C. D. Cress, R. A. DiLeo and R. P. Raffaelle (2009). "Carbon nanotubes for lithium ion batteries." Energy & Environmental Science 2(6): 638-654.

51. Gong, K., F. Du, Z. Xia, M. Durstock and L. Dai (2009). "Nitrogen-doped carbon nanotube arrays with high electrocatalytic activity for oxygen reduction." Science 323(5915): 760-764.

52. Wang, D., P. Song, C. Liu, W. Wu and S. Fan (2008). "Highly oriented carbon nanotube papers made of aligned carbon nanotubes." Nanotechnology 19(7): 075609.

53. Ago, H., K. Petritsch, M. S. Shaffer, A. H. Windle and R. H. Friend (1999). "Composites of carbon nanotubes and conjugated polymers for photovoltaic devices." Advanced Materials 11(15): 1281-1285.

54. Lv, R., F. Kang, W. Wang, J. Wei, X. Zhang, Z. Huang, J. Gu, K. Wang and D. Wu (2007). "Soft magnetic performance improvement of Fe‐filled carbon nanotubes by water‐assisted pyrolysis route." Physica Status Solidi (a) 204(3): 867-873.

55. Ci, L., S. M. Manikoth, X. Li, R. Vajtai and P. M. Ajayan (2007). "Ultrathick freestanding aligned carbon nanotube films." Advanced Materials 19(20): 3300-3303.

56. Brandrup, J., E. H. Immergut, E. A. Grulke, A. Abe and D. R. Bloch (1999). Polymer Handbook, Wiley New York.

57. Miller, R., H. Mark and N. Gaylord (1966). "Encyclopedia of Polymer Science and Technology." Vol. 4Wiley, New York, USA: 451.

58. Lodge, T. P. and P. Hiemenz (2007). "Polymer Chemistry." CRC Press Taylor & Francis Group.

59. Ciferri, A. (1982). Polymer Liquid Crystals, Elsevier.

60. Olabisi, O. and K. Adewale (1997). Handbook of Thermoplastics, CRC press.

61. Murray, G. (1997). Handbook of Materials Selection for Engineering Applications, CRC Press.

62. Huang, X. (2009). "Fabrication and properties of carbon fibers." Materials 2(4): 2369-2403.

63. Sung, M. G., K. Sassa, T. Tagawa, T. Miyata, H. Ogawa, M. Doyama, S. Yamada and S. Asai (2002). "Application of a high magnetic field in the carbonization process to increase the strength of carbon fibers." Carbon 40(11): 2013-2020.

64. Fitzer, E. (1990). Carbon fibres—present state and future expectations. Carbon Fibers Filaments and Composites, Springer: 3-41.

65. Donnet, J. and R. Bansal Carbon fibers, 1990, Dekker, New York.

66. Al-Saleh, M. H. and U. Sundararaj (2011). "Review of the mechanical properties of carbon nanofiber/polymer composites." Composites Part A: Applied Science and Manufacturing 42(12): 2126-2142.

67. Baughman, R. H., A. A. Zakhidov and W. A. de Heer (2002). "Carbon nanotubes--the route toward applications." Science 297(5582): 787-792.

68. Mordkovich, V. (2003). "Carbon nanofibers: a new ultrahigh-strength material for chemical technology." Theoretical Foundations of Chemical Engineering 37(5): 429-438.

69. Diouri, N. and M. Baitoul (2014). "Effect of carbon nanotubes dispersion on morphology, internal structure and thermal stability of electrospun poly (vinyl alcohol)/carbon nanotubes nanofibers." Optical and Quantum Electronics 46(1): 259-269.

70. Coleman, J. N., U. Khan, W. J. Blau and Y. K. Gun'ko (2006). "Small but strong: a review of the mechanical properties of carbon nanotube–polymer composites." Carbon 44(9): 1624-1652.

71. Raravikar, N. R., L. S. Schadler, A. Vijayaraghavan, Y. Zhao, B. Wei and P. M. Ajayan (2005). "Synthesis and characterization of thickness-aligned carbon nanotube-polymer composite films." Chemistry of Materials 17(5): 974-983.

72. Inagaki, M., Y. Yang and F. Kang (2012). "Carbon nanofibers prepared via electrospinning." Advanced Materials 24(19): 2547-2566.

73. Jeong, J., J. Moon, S. Jeon, J. Park, P. Alegaonkar and J. Yoo (2007). "Mechanical properties of electrospun PVA/MWNTs composite nanofibers." Thin Solid Films 515(12): 5136-5141.

74. Li, F., Y. Zhao and Y. Song (2010). "Core-Shell nanofibers: Nano channel and capsule by coaxial electrospinning."

75. Liu, K., Y. Sun, X. Lin, R. Zhou, J. Wang, S. Fan and K. Jiang (2010). "Scratch-resistant, highly conductive, and high-strength carbon nanotube-based composite yarns." ACS Nano 4(10): 5827-5834.

76. Liu, W., H. Zhao, Y. Inoue, X. Wang, P. D. Bradford, H. Kim, Y. Qiu and Y. Zhu (2012). "Poly (vinyl alcohol) reinforced with large-diameter carbon nanotubes via spray winding." Composites Part A: Applied Science and Manufacturing 43(4): 587-592.